C.P. No. 351
(18,306)
A.R.C. Technical Report

C.P. No. 351
(18,306)
A.R.C. Technical Report

MINISTRY OF SUPPLY

AERONAUTICAL RESEARCH COUNCIL

CURRENT PAPERS

Investigation of High Length/Beam Ratio Seaplane Hulls with High Beam Loadings

Hydrodynamic Stability Part 14

The Effect of a Tailored Afterbody on Stability and Spray Characteristics with Test Data on Model J

By

D. M. Ridland, A.F.R.Ae.S., G.I.Mech.E.

LONDON HER MAJESTY'S STATIONERY OFFICE

1957

SIX SHILLINGS NET

Report No. F/Res/249

October, 1955

C.P. No. 351

MARINE AIRCRAFT EXPERIMENTAL ESTABLISHMENT, FELIXSTOWE, SUFFOLK

INVESTIGATION OF HIGH LENGTH/BEAM RATIO SEAPLANE HULLS WITH HIGH BEAM LOADINGS

HYDRODYNAMIC STABILITY PART 14

THE EFFECT OF A TAILORED AFTERBODY ON STABILITY AND SPRAY CHARACTERISTICS WITH TEST DATA ON MODEL J

by

D. M. Ridland, A.F.R.Ae.S., G.I. Mech.E.

SUMMARY

The effects of a tailored afterbody on longitudinal stability, spray, directional stability and elevator effectiveness are deduced from the results of tests on two models of length/beam ratio 11, which were alike in every respect except that of afterbody shape; one afterbody was of standard form and the other was tailored.

It was found that tailoring the afterbody considerably improved stability characteristics, both longitudinal and directional, improved spray characteristics and slightly impaired elevator effectiveness.

The detailed test results for the tailored afterbody model are also included and discussed.

/ LIST OF CONTENTS

LIST OF CONTENTS

LIST OF TABLES

/ LIST OF FIGURES

LIST OF FIGURES

/ 1. INTRODUCTION

1. INTRODUCTION

This report is in two main sections; the first deals solely with the results of tests on the stability and spray characteristics of Model J, which is one of the series of models detailed in Reference 1, a list of which is given in Table I, while in the second these results are compared with those for Model A (the basic model of the series) to determine quantitatively the effects of a tailored afterbody on the hydrodynamic stability and spray characteristics of a high length/beam ratio hull.

2. THE STABILITY AND SPRAY CHARACTERISTICS OF MODEL J

The tests performed on Model J included the determination of longitudinal stability limits at C_{Δ_0} = 2.25 and 2.75 without slipstream and of the spray characteristics at these values of C_{Δ_0}, and an assessment of directional stability for C_{Δ_0} = 2.75 with the model constrained in roll. The techniques used in the tests and the presentation of results, together with the reasons for using them, are considered in References 1 and 2, though a brief summary is given below.

Figures are included showing the limits and there are a number of subsidiary diagrams. Where possible results have been presented non-dimensionally and curves for Model A have been included to facilitate comparison.

2.1. Description of Model

Model J has a length/beam ratio of 11 (the forebody being 6 beams in length and the afterbody 5 beams), an afterbody to forebody keel angle of 6°, a straight transverse step with a step depth of 0.15 beams and a tailored afterbody; it has no forebody warp and no step fairing. Full details are given in Reference 1 of considerations affecting the general design of the models, but hull lines and photographs of model J are given in Figures 1 and 2 respectively, while hydrodynamic and aerodynamic data are given in Tables II and III.

Model J was designed with the object of assessing the benefit, if any, to be obtained by applying the design procedure ("tailoring") laid down in Reference 14 to the afterbody of a hull of high length/beam ratio. Briefly, this procedure consists of determining the wake shape behind the forebody for a number of representative speed-attitude combinations (high and low attitudes at low, medium and high planing speeds), selecting the case with the least afterbody-wake clearance, and choosing an afterbody deadrise angle at each station such that the vertical separation of the keel and the wake is less than that of the wake and any other portion of the planing bottom at that station. The deadrise angles so obtained are then used as a basis for an afterbody with a smooth deadrise angle distribution, that resulting for Model J being shown in Figure 3 together with the standard afterbody deadrise angle distribution of Model A.

2.2. Description of Tests

2.2.1. General

All tests were made with one C.G. position, no slipstream, zero flap and at steady speeds only. The pitching moment of inertia of the model was 23.90 lb.ft.^{2} in all longitudinal stability tests.

2.2.2. Lift

Lift runs were made at constant speed with the model clear of the water, over a range of attitudes with $\eta = 0°$, and the effect of elevator was determined at five attitudes. The resulting curves are given in Figure 4.

2.2.3. Longitudinal Stability

Longitudinal stability tests were made by towing the model from the wing tips on the lateral axis through the centre of gravity, the model

/ being

being free in pitch and heave. The value of the elevator setting was selected before each run, and the model towed at constant speed. The angle of trim was noted in the steady condition, and if the model proved stable at the speed selected it was given nose-down disturbances to determine whether instability could be induced, the amount of disturbance given to cause instability being in the range 0-14°. Stability limits were built up by these methods, the disturbed limits representing the worst possible case. Tests were carried out with C_{Δ_0} = 2.25 and 2.75 and the corresponding trim curves and stability limits are given in Figures 5 - 8. The limits for the different values of C_{Δ_0} are plotted together for comparison on a C_v base in Figure 9, which includes the corresponding curves for Model A. Figures 10 and 11 show load coefficient curves calculated from the lift and trim curves.

When steady porpoising occurred, either with or without disturbance, the amplitude was noted, amplitude for this purpose being defined as the difference between the maximum and minimum trims attained in the oscillation. These amplitudes are plotted in Figures 12 and 13, for the various cases concerned.

2.2.4. Spray and Wake Formation

Photographs were taken of the spray, from three different positions, over a range of speeds and with elevators set at -8°. A number of these photographs are reproduced in Figures 16 to 19. They have been used to determine the projections of the spray envelopes on the plane of symmetry of the model at the different values of C_{Δ_0}, and these projections are plotted together with those for Model A in Figure 20. This method of plotting differs from that originally proposed (Reference 1) but is felt to be more realistic. The absence of projections orthogonal to these, which cannot be obtained from the photographs is not serious since the photographs enable the positions of the spray blisters to be judged qualitatively, and in any case the curves are intended for comparison purposes rather than for absolute measurements. It should be noted that in plotting the projections velocity spray has in general been ignored.

In addition to the spray photographs, photographs of the wake region were taken from two different positions and are reproduced in Figures 14 and 15. These photographs covered a range of speeds and elevator settings, the combinations being selected to give the maximum possible variation of wake formation and position relative to the afterbody in the stable planing region.

2.2.5. Directional Stability

In the directional stability tests, the model was pivoted universally at the C.G. and then separately constrained in roll so that it was free in pitch, yaw and heave. The roll constraint was introduced after it had been ascertained on a previous model (Reference 3) that it had no appreciable effect on directional stability. The model was towed from the C.G. and moments to yaw the model were applied by means of strings attached to the wing tips and in the same horizontal plane as the C.G.

Steady speed runs were made with elevators set at 0 and - 4 degrees, the model being yawed up to at most 18 degrees and the values of yaw giving equilibrium determined by the operator by assessment of the direction of the resulting hydrodynamic moment on the model. The occurrence of very high drag forces at large angles of yaw at high speeds made it impossible to investigate some regions. The elevator setting of zero degrees chosen initially was changed to -4 degrees about halfway through the tests in an attempt to reduce the porpoising induced by yawing the model with the zero degree setting. Apart from the reduction of porpoising, this elevator change should have negligible effect on the directional stability characteristics of the model (Reference 3). The value of C_{Δ_0} in these tests was 2.75 and the resulting stability diagram is given together with the corresponding diagram for Model A in Figure 21. As it had been previously found (Reference 5) that load changes have little effect on directional stability it was not considered necessary to investigate directional characteristics at both values of C_{Δ_0}.

/ Similar

Similar tests with breaker strips fitted were not carried out on this model, as it has been found that their effect is only to remove the outer lines of equilibrium at the higher speeds (Reference 1).

2.2.6. Elevator Effectiveness

Curves of elevator effectiveness calculated from the longitudinal stability diagrams are given in Figures 22 and 23. The final curves of mean elevator effectiveness are compared with those for Model A in Figures 25.

2.3. Discussion of Results

The lift curves (Figure 4) do not vary substantially from those for the basic model, with which identical wing and tail units were used, but both the elevator and attitude ranges have been extended to correspond to the large trim ranges of which this model is capable. The small but rather sharp change in slope of the lift curves occurring about $\alpha_K = 7^0$ is probably due to the high deadrise afterbody.

The longitudinal stability of the model is fairly good. In the undisturbed case at $C_{\Delta_0} = 2.25$ (Figure 5,) , although a stable take-off path is available, there is a region of low amplitude porpoising just above hump speed which, while not classified as instability by the definitionused for these tests[1], indicates that a small increase in load would produce an unstable band there. This in fact has happened at $C_{\Delta_0} = 2.75$ (Figure 7), but the instability is found only over a narrow speed band and should not therefore cause much trouble during take-off. At each weight a wide stable trim range is available over most of the planing range of speeds and the region of upper limit instability is so small as to be negligible in a practical case.

The effect of disturbance (Figures 6 and 8) is to produce a vertical band of instability across the take-off path at the lower weight, and to widen the existing band at the higher weight. In both cases the high speed ends of the lower limits are raised slightly, but the upper limit unstable regions are unaltered and stability generally, though worse than in the undisturbed case, still remains reasonable. Porpoising amplitudes (Figures 12 and 13) are increased by disturbance, but not greatly as they are already large in the undisturbed case, and, following the application of suitable disturbances in the high speed, lower limit region, the model leaves the water during each porpoising cycle.

The effect of the increased load on stability is to cause a general deterioration. The stability limits, both undisturbed and disturbed (Figure 9), are moved bodily up the speed scale by about one unit of C_V, while hump trim, which is high initially, is increased by approximately one degree; trim in general is raised by about one degree, but the character of the trim curves remains unchanged. Porpoising amplitudes, both undisturbed and disturbed, show a marked increase with increase in weight.

The load coefficient curves of Figures 10 and 11 can be used to estimate flying speeds, but it should be noted that no allowance for ground effect has been made in them.

Photographs of flow in the wake (Figures 14 and 15) are included to show the position of the afterbody relative to the wake in representative positions in the undisturbed stable planing region so that its association with upper limit undisturbed stability in particular, and disturbed stability in general, can be investigated. It may be recalled that the aim of the tailored afterbody design technique is to ensure good afterbody ventilation, thereby eliminating, to a large extent, instability which is directly attributable to poor ventilation. For this to happen there must be adequate clearance between the afterbody chines and trough walls so that the inflowing air suffers no impedance. This is obtained with the present design as can be seen in Figure 14(d) which illustrates a high speed, high attitude

/ configuration

configuration, stable both with and without disturbance, at $C_{\Delta_0} = 2.25$, in a region where upper limit instability might well be expected. The rear step is immersed, but apart from the rearmost $\frac{1}{2}$ beam the chines are well clear. Similar remarks may be applied to Figure 15(d) which is for a comparable configuration at $C_{\Delta_0} = 2.75$. Although the attitude here is lower than in the previous case the aft step is planing and, as before, chine clearance is adequate.

On examining the remaining photographs of Figure 14 it can be seen that in (a) and (b) the afterbodies are planing while in (c) and (e) they are clear. From the relevant stability diagram, (a) and (c) are stable following the application of a disturbance, while (b) and (e) are unstable, the latter violently so. On this basis therefore there is no relationship between the planing of the afterbody and disturbed instability. Similar remarks can be applied to the remaining photographs for the higher weight case in Figure 15. Here only (c) remains stable after the application of a disturbance and only in (a) is the afterbody planing.

Two main conclusions may be drawn from the photographs as a whole. The first is that the afterbody chines are in every case well clear of the trough wall, so ventilation from this source should be adequate, and the second is that all chine wetting is confined to within $\frac{1}{2}$ beam of the aft step, so that as far as the planing range of speeds is concerned, the chines forward of this point could be faired, thereby further improving the ventilation. It may be remarked that in the present case the chine clearance may be excessive. This will in no way affect the conclusions drawn with respect to the tailored afterbody, but in a specific design it will clearly be advantageous to keep afterbody deadrises as small as possible in order to maintain maximum afterbody volume.

Figures 16 - 19 show the spray formation at two weights with one elevator setting ($\eta = -8^\circ$), mainly over the displacement range of speeds. The spray characteristics of this model are acceptable at the lower weight; velocity spray strikes the undersurface of the mainplane at $C_v = 3.63$ and 4.09 while the tailplane is, for practical purposes, at all times clear. The increase in weight however, causes a rapid deterioration; heavier velocity spray, and occasionally main spray, hits the wing undersurface over a greater speed range than at the lower weight and the tailplane is affected by broken spray from the afterbody. This exaggerated afterbody spray occurs at both loadings at about $C_v = 3$ and can be clearly seen in Figures 16 and 18. It is met over a very limited speed range, however, and should not be significant from the design point of view. The effect of weight change on both main spray and afterbody spray is shown clearly in Figure 20, in which the projections of the spray envelopes on the plane of symmetry of the model are plotted.

Details of the interpretation of the directional stability diagram (Figure 21) have already been given in Reference 1, and only a few additional remarks will be made here. The directional stability of Model J appears to be very good. Apart from the short speed range just above $C_v = 3$ where unstable equilibrium is met and where the maximum inherent yaw angle is limited to 3 degrees, it should be easy to control this hull form directionally from $C_v = 2.6$ upwards. In particular, the absolute inherent stability at hump speed ($C_v = 4.5$) should be noted. In the high speed region only very small moments were necessary to initiate or curtail a yaw and on several occasions when the nominal limit in yaw for the test was exceeded, only moderate restraining moments were necessary.

The diagrams of elevator effectiveness (Figures 22, 23 and 25) show that with increase of load there is a decrease in effectiveness which is almost independent of speed within the range covered.

3. THE EFFECTS OF A TAILORED AFTERBODY ON STABILITY AND SPRAY CHARACTERISTICS

3.1. General

In this section of the report the test results for Model J already considered are compared with similar results for the basic model of the series, Model A. A detailed account of the tests on Model A is given in Reference 3, but

/ the

the main results are incorporated in the relevant figures of the present report. The two models were identical except in respect of the afterbody deadrise angle distributions and these are compared in Figure 3; it is seen that large increases in deadrise result from the application of the afterbody tailoring technique.

The same test methods were employed consistently throughout the investigation and they are discussed fully, together with the presentation of results, in References 1 and 2; a résumé of the details has already been given in Section 2 of this report. All the tests now under consideration were made with zero flap, no slipstream, one C.G. position and, except for the directional stability assessment, at the two beam loadings C_{Δ_0} = 2.75 and 2.25; directional tests were made only at C_{Δ_0} = 2.75.

3.2. Longitudinal Stability

The effects of a tailored afterbody on the longitudinal stability limits are shown in Figure 9 where both undisturbed and disturbed limits for Models A and J are compared. In the undisturbed case at both loadings, tailoring the afterbody has resulted in a considerable increase in the available stable planing region; this improvement has been brought about in each case primarily by the reduction and movement to higher speeds and attitudes of the upper limit unstable region. Higher attitudes are attained generally and in particular, the lower limits for Model J extend to higher attitudes; at C_{Δ_0} = 2.25 maximum lower critical trim has been raised by 2 degrees, while at C_{Δ_0} = 2.75 the low speed neck of instability is similarly raised by about 2 degrees.

The effect of load change on the undisturbed limits is only modified slightly by the tailored afterbody, the general form of each set of limits remaining unchanged at each weight. The raising of the lower limit with increase of weight is reduced slightly by tailoring and the upper limit, while being found at higher speeds as in the basic model case, is not raised by weight increase.

In the disturbed case the results of tailoring the afterbody are very similar in detail to those of the undisturbed case; the improvement is much greater however, with the available stable planing region being almost doubled. The general relationships between the two sets of limits are the same from weight to weight and it is clear that the effects of load changes are unaltered by the tailored afterbody.

As the improvement or increase in the stable planing region obtained by tailoring the afterbody is greater in the disturbed than in the undisturbed cases, it follows that the resistance of the model to disturbance has been greatly increased i.e. the general level of critical disturbances has been raised (Reference 15). Examination of Figure 9(b) indicates that this effect is greatest at high attitudes, being progressively reduced with decrease of attitude, until it becomes negligible in the high speed, lower limit regions.

An explanation of disturbed instability in terms of afterbody suctions has been offered by Gott and upheld by recent experience [15, 16]. Accepting this it follows that, as some disturbed instability is still obtained with the tailored afterbody, there must remain some regions of afterbody suction i.e. the design technique is not quite correct or it has been inadequately applied. In view of the gains obtained and on general physical ground, there is no reason for suspecting the technique, so the application must be at fault. An obvious source of suction on Model J is the transverse vertical step, the space immediately behind which is normally a low pressure region. If this step were streamlined or ducted and all afterbody suctions were thereby alleviated, one might expect complete elimination of disturbed instability. The effects of such modifications on upper limit undisturbed instability could hardly be detrimental and, as with the present tailored afterbody only negligible upper limit instability is met, the issue is of secondary importance. In any practical design incorporating a tailored afterbody, then, the main step should be either streamlined or ducted.

During the tests just considered the pitching moments of inertia of Models A and J were 22.90 and 23.90 lb.ft.^{2} respectively. By the conclusions

/ of

of Reference 2, moment of inertia increases of up to 40% have no appreciable effect on the limits, so the difference in moment of inertia values does not affect the foregoing discussion.

The effects of a tailored afterbody on trim are illustrated in Figure 24, where trim curves for $\eta = 0^{\circ}$, which have been taken as typical, are compared. At both loadings there is an increase in trim in the static floating condition of $1\frac{1}{2}^{\circ}$, which value increases over the displacement range of speeds, becoming 2° at the hump, and the curves tend to run just below those for the unmodified afterbody in the planing speed range. This positioning of the tailored afterbody trim curves below those of the standard afterbody is general over the planing speed range of trims, the effect being slightly greater at the higher weight than at the lower, and is what one would expect following a relief of suctions in the tailored afterbody case.

Amplitudes of porpoising (Figures 12 and 13 and Reference 3) are not materially affected in the undisturbed case at either weight by tailoring the afterbody; in the disturbed case, however, tailoring reduces amplitudes slightly at the lower weight and increases them at the higher weight.

3.3. Wake formation

Consideration has already been given in Section 2 to the photographs of flow in the wake behind the tailored afterbody. A re-examination of these photographs in conjunction with the corresponding ones for the basic model gives a general quantitative impression of the amount of wake-chine clearance, which is considerable, actually obtained by applying the tailoring technique to an afterbody. Detailed comparison is only possible in isolated cases because of the representative nature of the photographs and little more is to be learned from this source.

3.4. Spray

The effects of a tailored afterbody on spray are shown at both loadings in Figure 20. At $C_{\Delta_o} = 2.25$ the projections for both models are continuous and show that in each case the main planes were more or less clear of spray. At positive values of C_X however, in which region the spray envelope corresponds to low displacement speeds, the curve for the tailored afterbody model is well below that for the basic model, indicating a useful reduction in maximum spray height in the vicinity of the propeller plane; at higher speeds there is negligible difference between the spray profiles. The peculiar afterbody spray formation of Model J, which occurs at both weights, has been mentioned in Section 2.3 and should not be significant because of its short duration during take-off or landing. At the higher loading, $C_{\Delta_o} = 2.75$, the improvement in low speed spray characteristics obtained with the tailored afterbody is verified and appears to be unchanged in magnitude. The general deterioration due to the weight increase is obvious in that the profiles are now discontinuous, indicating that main spray or heavy velocity spray struck the mainplane.

The improvement in spray characteristics obtained with the tailored afterbody follows directly from the consequent increased attitudes at a given elevator setting. There will be minor changes in draught, but these should only have a small effect on spray. The movement backward of the spray origin, at a given speed, with the increase in attitude can be seen when comparing the individual spray photographs and is considerable at $C_V = 3$ and 4 at both weights.

3.5. Directional Stability

Directional stability diagrams for the two models are compared in Figure 21. It can be seen that tailoring the afterbody has resulted in a considerable overall improvement in directional characteristics. At pre-hump speeds, where attitudes are high and a slight yaw could cause wing dropping, Model J is inherently stable and it is at these speeds that the greatest improvement over the basic model is obtained. At the higher speeds both hull forms should be easily controllable at small angles of yaw but, whereas the basic

/model

model shows a violent tendency to increase yaw when the eqilibrium line is exceeded, the reverse is true of the tailored afterbody model; the unstable equilibrium line of the basic model has been replaced by a line of weak stable equilibrium and the tailored hull in consequence should be controllable at angles of yaw in excess of 10°. Such a characteristic would be most useful in cross wind landings.

3.6. Elevator Effectiveness

The effects of a tailored afterbody on mean elevator effectiveness are shown in Figure 25. At the lower loading the curve for Model J lies below that for the basic model and the separation increases with speed, though at no time is it great; at the higher loading there is little practical difference between the two models. Perhaps the most significant effect that tailoring the afterbody has on elevator effectiveness is the reduction, about one third, in the effect of of load change.

4. CONCLUSIONS

The results of the present investigation show that considerable gains in hydrodynamic stability and spray characteristics are obtained by applying the tailoring design technique to the afterbody of a high length/beam ratio flying boat hull. The detailed effects of tailoring the afterbody (but not the main step) are

(i) to increase maximum lower critical trim and slightly reduce the speed at which it occurs,

(ii) to increase trim generally and, in particular, to increase hump trim and the maximum trim available with normal elevators,

(iii) to raise the upper undisturbed stability limit while at the same time reducing the extent of the upper unstable region,

(iv) to slightly reduce the effect of load on the position of the lower stability limit,

(v) to increase resistance to disturbance,

(vi) to increase disturbed amplitudes of porpoising at high loadings and to slightly decrease them at the low loadings,

(vii) to move the spray origin backwards, giving rise to improved spray characteristics (associated with (ii)),

(viii) to improve considerably directional qualities from high displacement speeds upwards and

(ix) to reduce the effect of load on elevator effectiveness.

The effects listed above are, except where otherwise indicated, independent of load.

The tailored afterbody design technique has been proved efficacious in the case of a high length/beam ratio hull by the present tests, but in a practical design case the application of the technique should include the modification of main step and chines. The main step should be considered in conjunction with the afterbody; it should be faired so as to induce a suitable airflow under the afterbody, or ducted and have an independent air supply. The afterbody chines are unwetted except near the rear step, so they could be faired and this would not only further aid afterbody ventilation but would reduce aerodynamic drag. Finally, the afterbody deadrise angles should be sufficient but not excessive as useful afterbody volume would be lost thereby.

/ ADVANCE DISTRIBUTION LIST

LIST OF SYMBOLS

b	beam of model
d	draught
C_L	lift coefficient = $L/\frac{1}{2}\rho SV^2$ (L = lift, ρ = air density).
C_V	velocity coefficient = $V/\sqrt{gb}$
C_Δ	load coefficient = Δ/wb^3 (Δ = load on water and w = weight per unit volume of water)
C_{Δ_o}	load coefficient at $V = 0$
C_X	longitudinal spray coefficient = x/b
C_Y	lateral spray coefficient = y/b
C_Z	vertical spray coefficient = z/b
	{(x,y,z) co-ordinates of points on spray envelope relative to axes through step point}
S	gross wing area
V	velocity
α_K	keel attitude
η	elevator setting
ψ	angle of yaw

/ LIST OF REFERENCES

LIST OF REFERENCES

No.	Author(s)	Title
1	D. M. Ridland J. K. Friswell A. G. Kurn	Investigation of High Length/Beam Ratio Seaplane Hulls with High Beam Loadings: Hydrodynamic Stability Part 1: Techniques and Presentation of Results of Model Tests. Current Paper 201. September 1953.
2	J. K. Friswell A. G. Kurn D. M. Ridland	Investigation of High Length/Beam Ratio Seaplane Hulls with High Beam Loadings: Hydrodynamic Stability Part 2: The Effect of Changes in the Mass, Moment of Inertia and Radius of Gyration on Longitudinal Stability Limits. Current Paper 202. September 1953.
3	D. M. Ridland J. K. Friswell A. G. Kurn	Investigation of High Length/Beam Ratio Seaplane Hulls with High Beam Loadings: Hydrodynamic Stability Part 3: The Stability and Spray Characteristics of Model A. M.A.E.E. Report F/Res/237. February 1954.
4	D. M. Ridland A. G. Kurn J. K. Friswell	Investigation of High Length/Beam Ratio Seaplane Hulls with High Beam Loadings: Hydrodynamic Stability Part 4: The Stability and Spray Characteristics of Model B. M.A.E.E. Report F/Res/238. March 1954.
5	J. K. Friswell D. M. Ridland A. G. Kurn	Investigation of High Length/Beam Ratio Seaplane Hulls with High Beam Loadings: Hydrodynamic Stability Part 5: The Stability and Spray Characteristics of Model C. M.A.E.E. Report F/Res/239. October 1953.
6	D. M. Ridland	Investigation of High Length/Beam Ratio Seaplane Hulls with High Beam Loadings: Hydrodynamic Stability Part 6: The Effect of Forebody Warp on Stability and Spray Characteristics. Current Paper 203. May 1954.
7	J. K. Friswell	Investigation of High Length/Beam Ratio Seaplane Hulls with High Beam Loadings: Hydrodynamic Stability Part 7: The Stability and Spray Characteristics of Model D. M.A.E.E. Report F/Res/241. November 1953.
8	D. M. Ridland	Investigation of High Length/Beam Ratio Seaplane Hulls with High Beam Loadings: Hydrodynamic Stability Part 8: The Stability and Spray Characteristics of Model E. M.A.E.E. Report F/Res/242. December 1953.
9	A. G. Kurn	Investigation of High Length/Beam Ratio Seaplane Hulls with High Beam Loadings: Hydrodynamic Stability Part 9: The Stability and Spray Characteristics of Model F. M.A.E.E. Report F/Res/243. February 1954.

LIST OF REFERENCES (Contd.)

No.	Author(s)	Title
10	D. M. Ridland	Investigation of High Length/Beam Ratio Seaplane Hulls with High Beam Loadings: Hydrodynamic Stability Part 10: The Effect of Afterbody Length on Stability and Spray Characteristics. Current Paper 204. August 1954.
11	D. M. Ridland A. G. Kurn J. K. Friswell	Investigation of High Length/Beam Ratio Seaplane Hulls with High Beam Loadings: Hydrodynamic Stability Part 11: The Stability and Spray Characteristics of Model G. M.A.E.E. Report F/Res/246. April 1954.
12	J. K. Friswell D. M. Ridland A. G. Kurn	Investigation of High Length/Beam Ratio Seaplane Hulls with High Beam Loadings: Hydrodynamic Stability Part 12: The Stability and Spray Characteristics of Model H. M.A.E.E. Report F/Res/247. February 1954.
13	D. M. Ridland	Investigation of High Length/Beam Ratio Seaplane Hulls with High Beam Loadings: Hydrodynamic Stability Part 13: The Effect of Afterbody Angle on Stability and Spray Characteristics. Current Paper 236. February 1955.
14	K. M. Tomaszewski A. G. Smith	Some Aspects of the Flow round Planing Seaplane Hulls or Floats and Improvement in Step and Afterbody Design. M.A.E.E. Note F/TN/4. September 1954.
15	D. M. Ridland	Investigation of High Length/Beam Ratio Seaplane Hulls with High Beam Loading: Hydrodynamic Stability Part 21: Some Notes on the Effects of Waves on Longitudinal Stability Characteristics. M.A.E.E. Report F/Res/257. August 1955.
16	J. P. Gott	Interference between Airflow and Water Flow in Seaplane Tank Testing. R.A.E. T.N. Aero 1460. July 1944

/ TABLE I

TABLE I

Models for hydrodynamic stability tests

Model	Forebody warp	Afterbody length	Afterbody-forebody keel angle	Step form	To determine effect of
	degrees per beam	beams	degrees		
A	0	5	6	Unfaired transverse. Step depth 0.15 beam.	Forebody warp
B	4	5	6		
C	8	5	6		
D	0	4	6		Afterbody length
A	0	5	6		
E	0	7	6		
F	0	9	6		
G	0	5	4		Afterbody angle
A	0	5	6		
H	0	5	8		
A	0	5	6		Tailored afterbody
J	0	5	6		
A	0	5	6		Interaction of parameters
B	4	5	6		
E	0	7	6		
H	0	5	8		
K	4	5	8		
L	4	7	6		
M	0	7	8		
N	4	7	8		

/ TABLE II

TABLE II

MODEL J

HYDRODYNAMIC DATA

Beam at step (b)	0.475'
Length of forebody (6b)	2.850'
Length of afterbody (5b)	2.375'
Forebody deadrise at step	25°
Forebody warp (per beam)	0°
Afterbody form	tailored (See Figure 3 for afterbody deadrise angle distribution.)
Afterbody angle	6°
Pitching moment of inertia	23.90 lb.ft.^{2}

/ TABLE III

TABLE III

Model Aerodynamic data

Mainplane		
Section		Gottingen 436 (mod.)
Gross area		6.85 sq. ft.
Span		6.27 ft.
S.M.C.		1.09 ft.
Aspect ratio		5.75
Dihedral	on 30% spar axis	3° 0'
Sweepback	on 30% spar axis	4° 0'
Wing setting (root chord to hull datum)		6° 9'
Tailplane		
Section		R.A.F. 30 (mod.)
Gross area		1.33 sq. ft.
Span		2.16 ft.
Total elevator area		0.72 sq. ft.
Tailplane setting (root chord to hull datum)		2° 0'
Fin		
Section		R.A.F. 30
Gross area		0.80 sq. ft.
Height		1.14 ft.
General		
* C.G. position		
distance forward of step point		0.237 ft.
distance above step point		0.731 ft.
* $\frac{1}{4}$ chord point S.M.C.		
distance forward of step point		0.277 ft.
distance above step point		1.015 ft.
* Tail arm (C.G. to hinge axis)		3.1 ft.
* Height of tailplane root chord L.E. above hull crown		0.72 ft.

* These distances are measured either parallel to or normal to the hull datum.

FIG. 1.

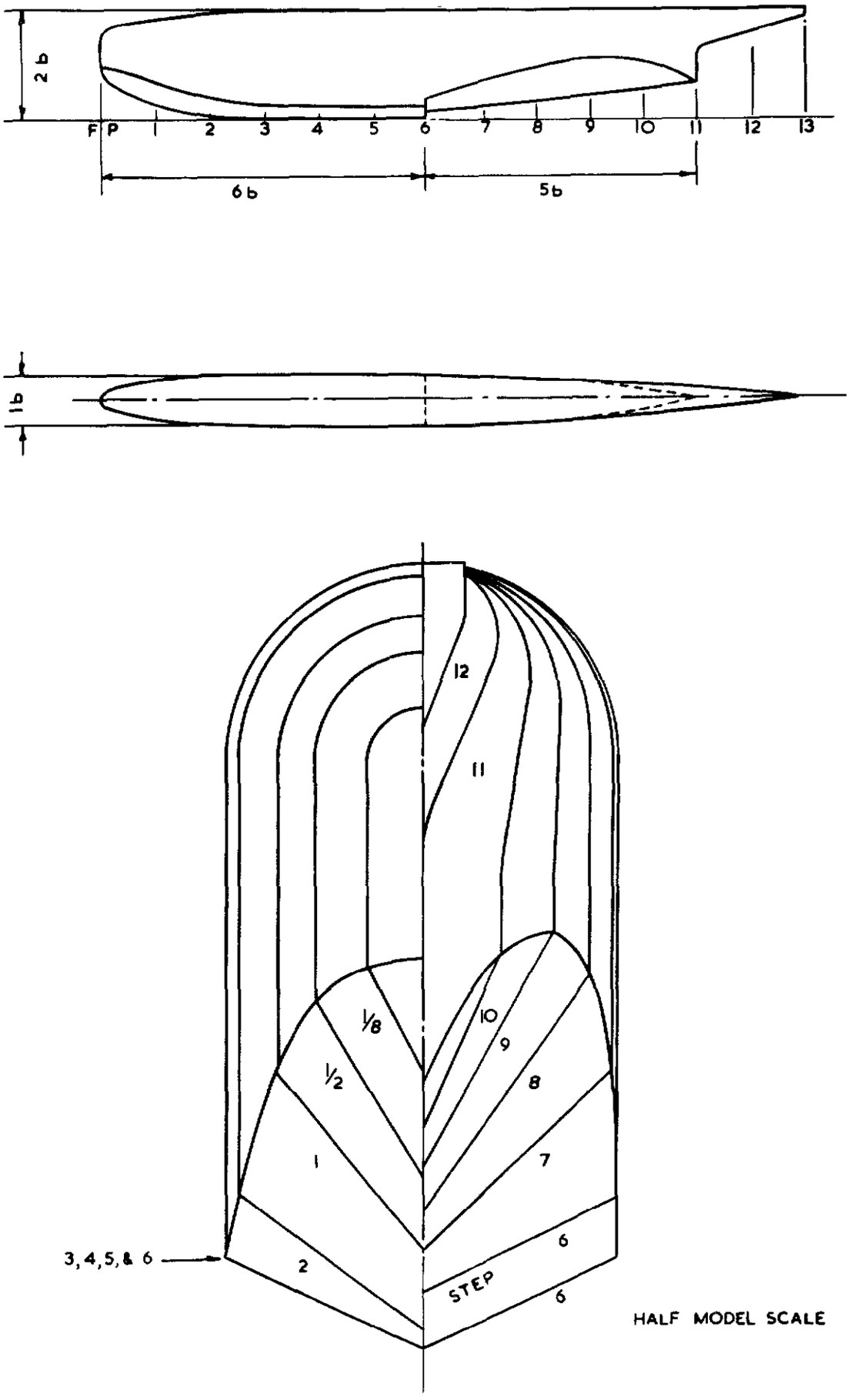

MODEL J

HULL LINES

FIG. 2.

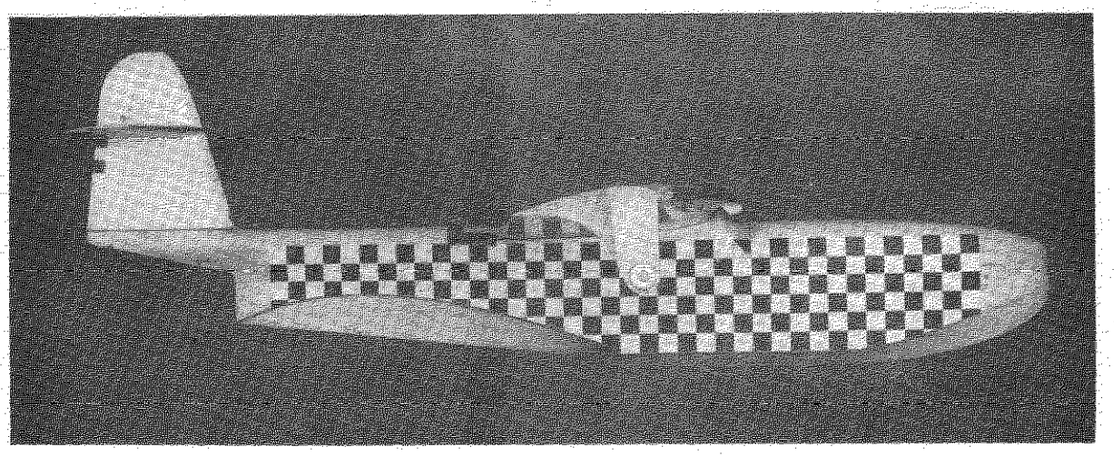

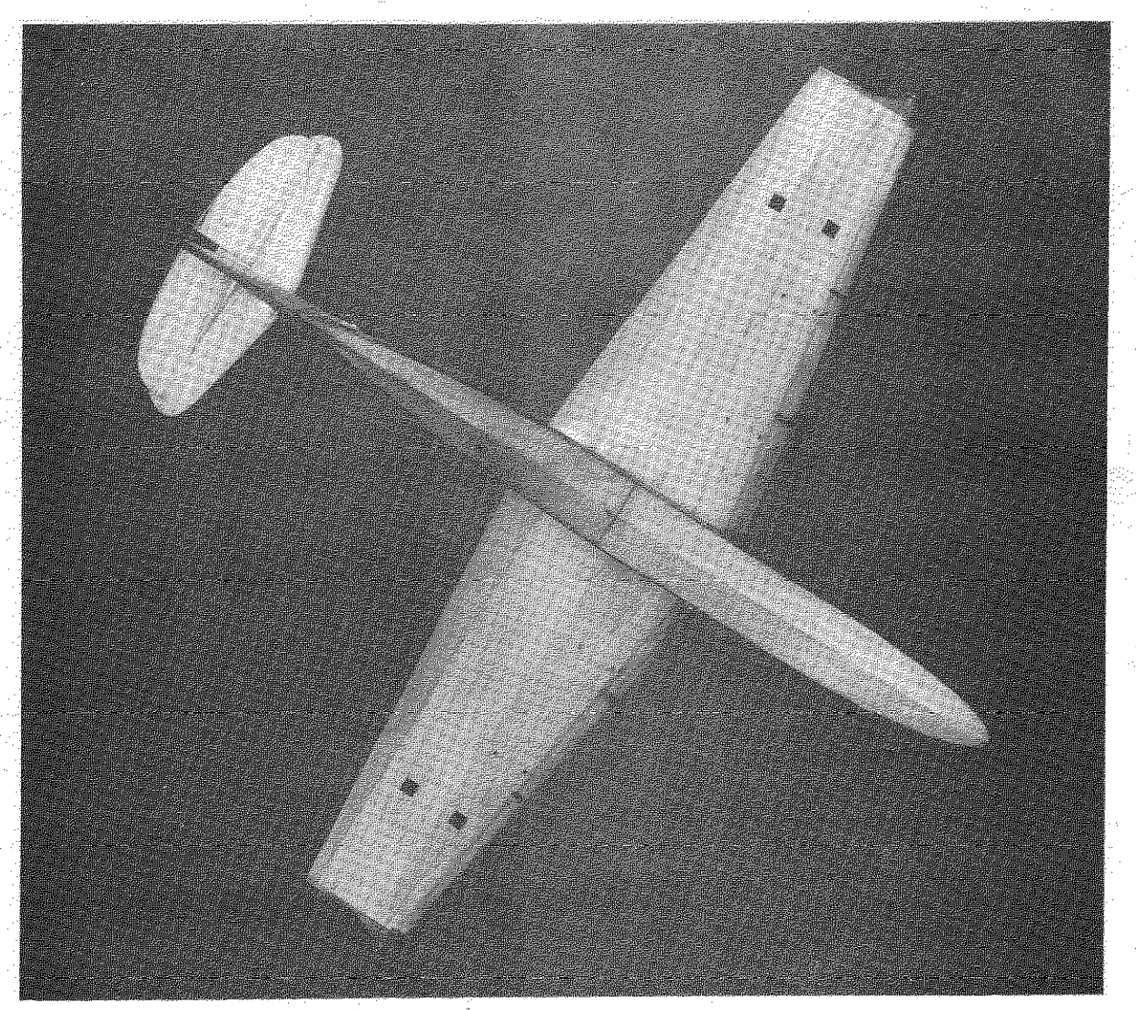

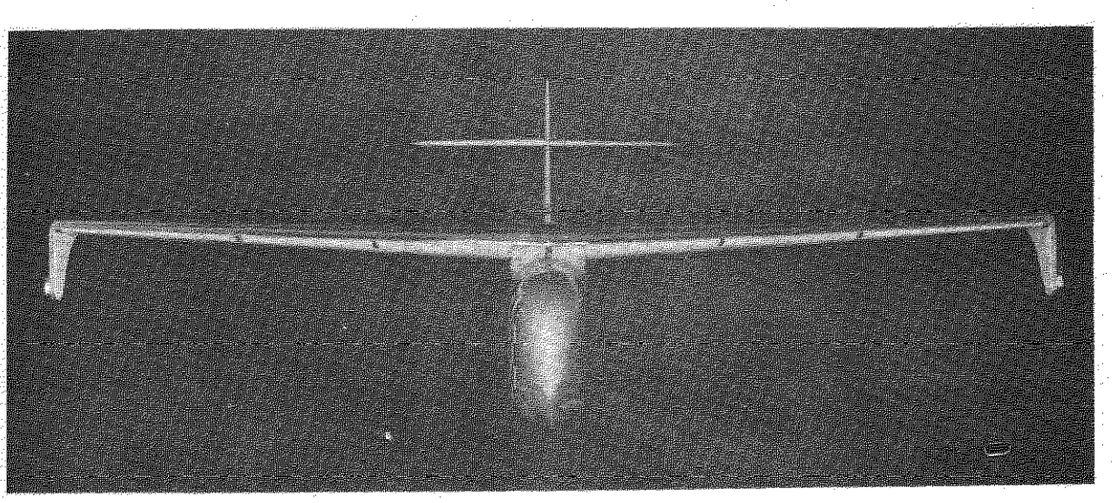

PHOTOGRAPHS OF MODEL J

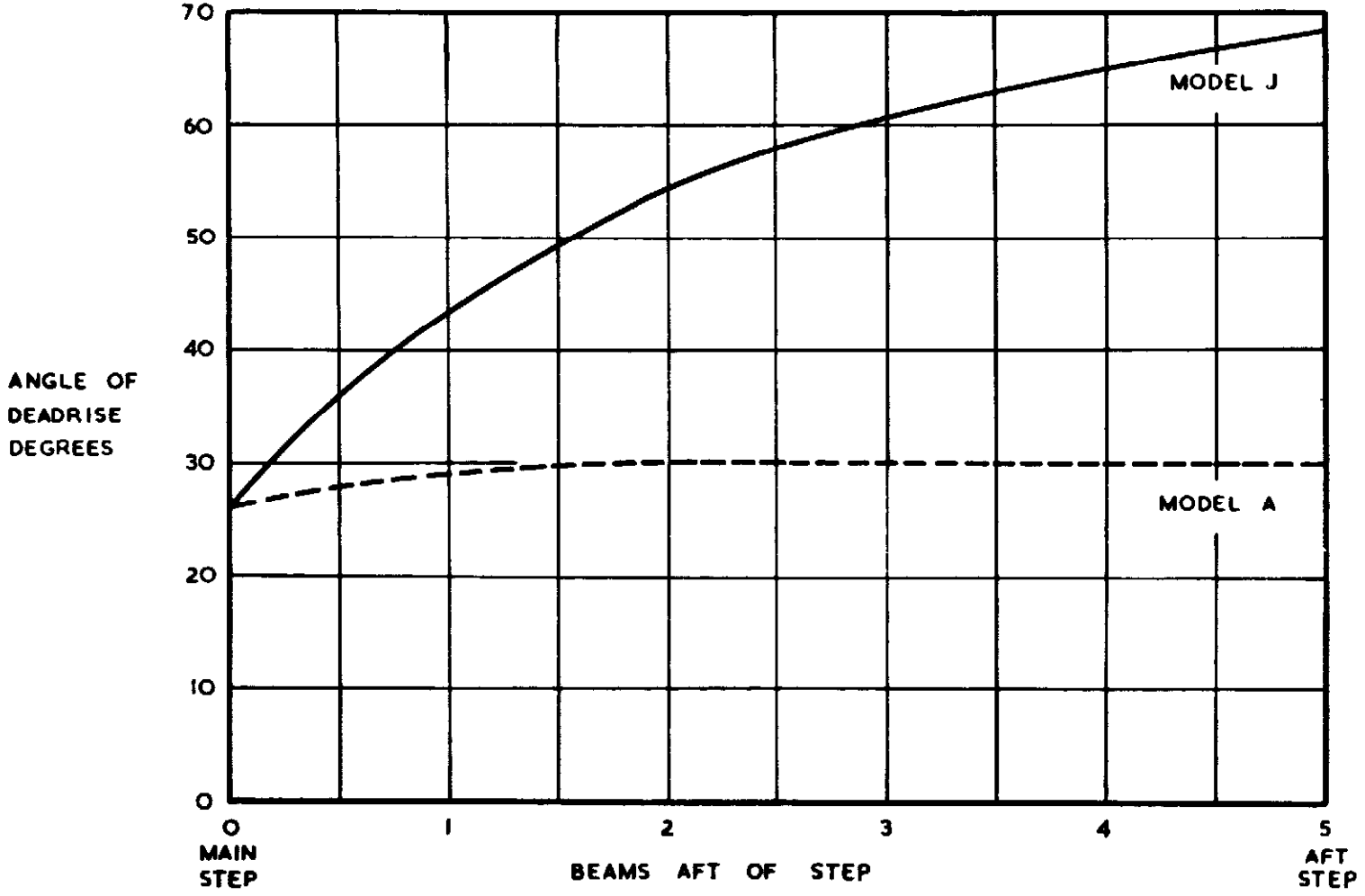

FIG. 3.

AFTERBODY DEADRISE ANGLE DISTRIBUTIONS.

FIG. 4.

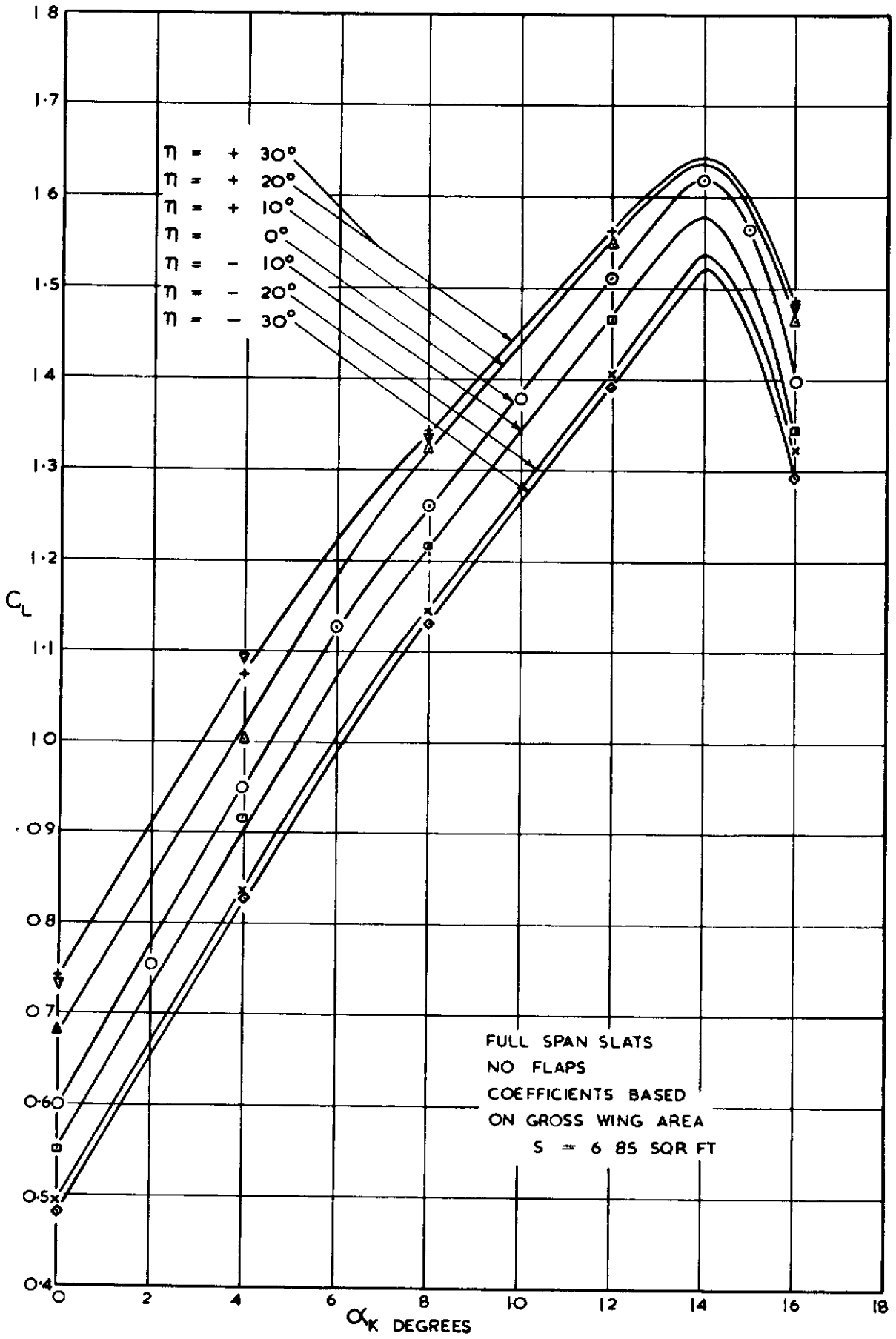

MODEL J

LIFT CURVES WITHOUT SLIPSTREAM

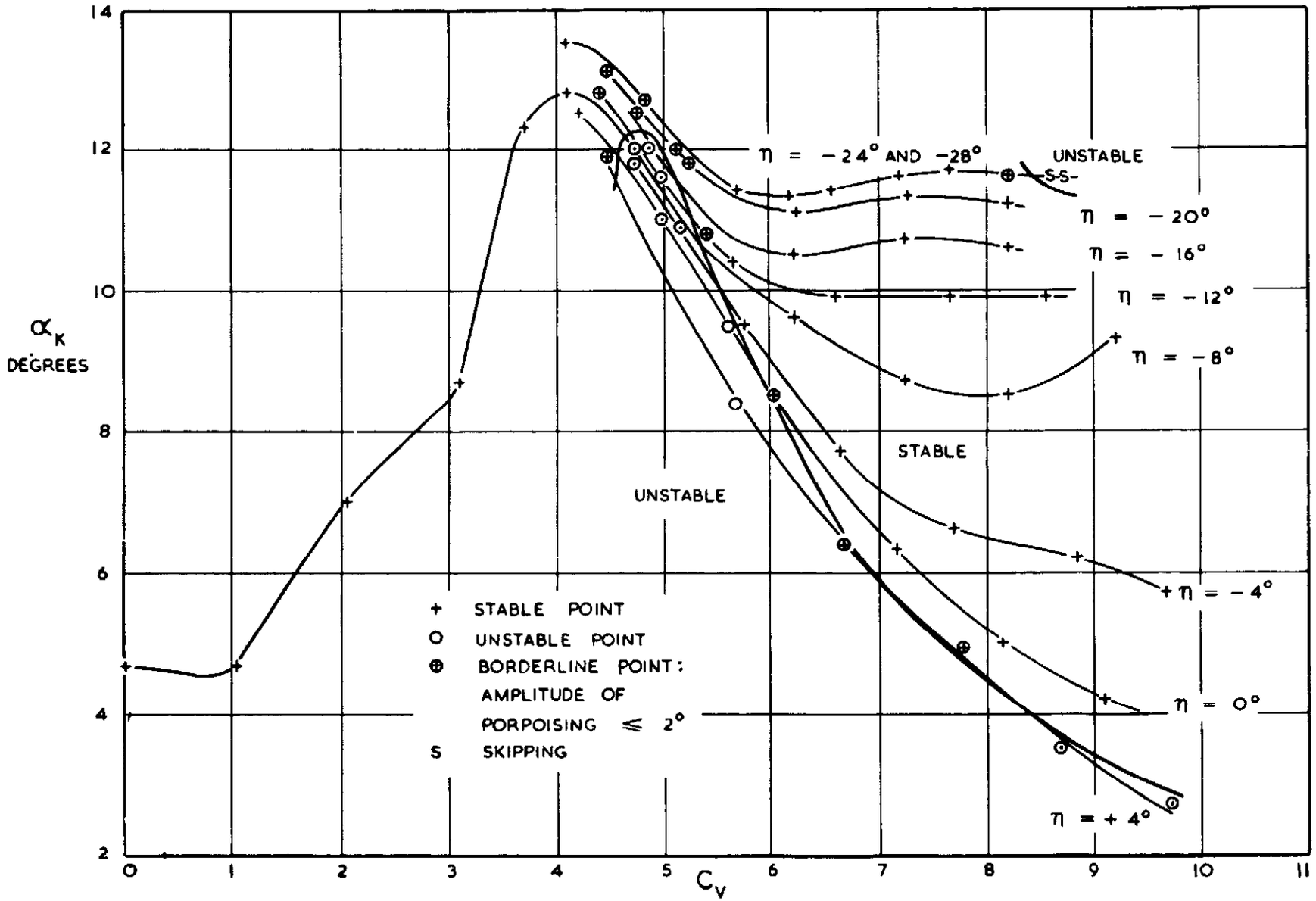

MODEL J
LONGITUDINAL STABILITY WITHOUT DISTURBANCE, C = 2·25

FIG.5.

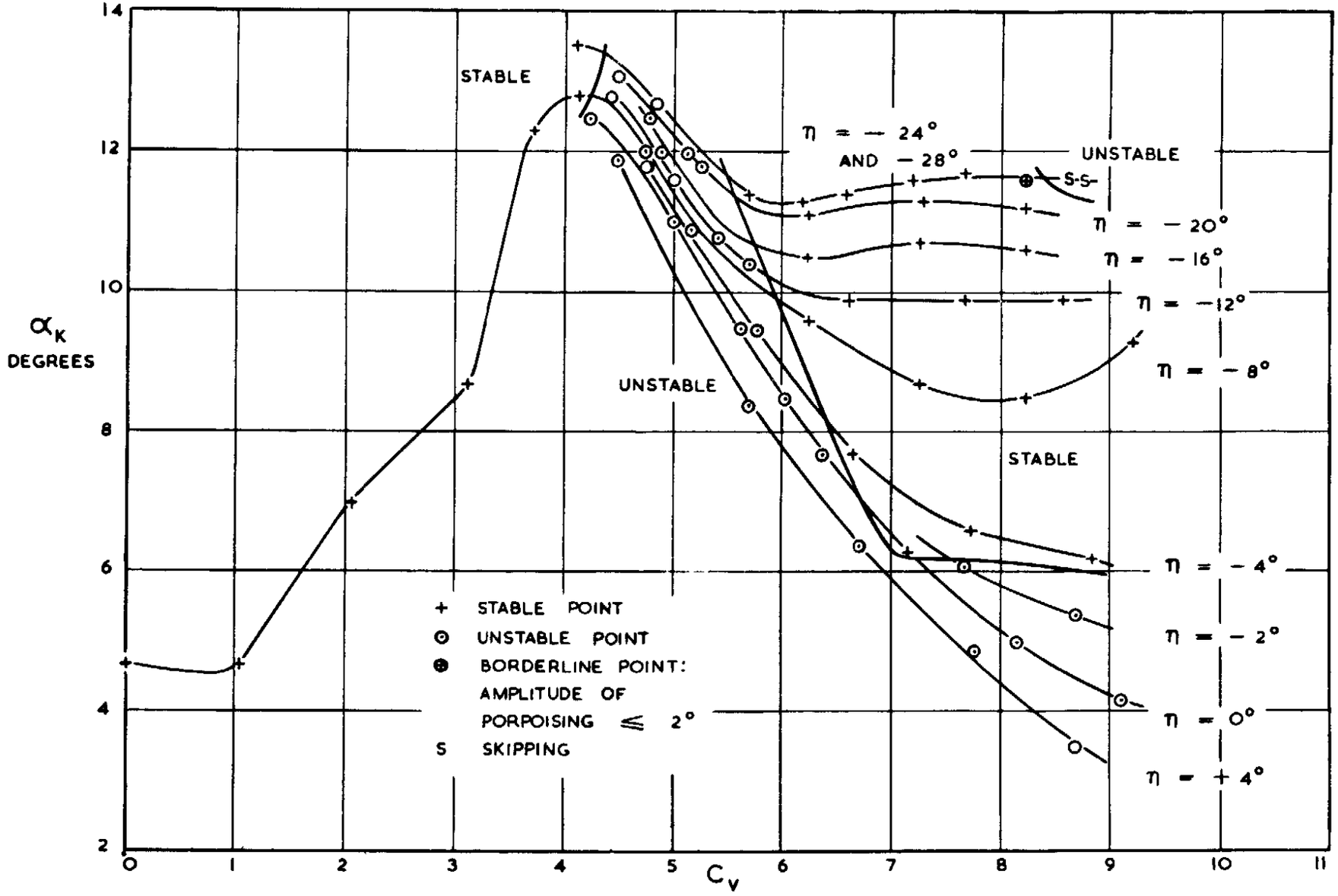

MODEL J
LONGITUDINAL STABILITY WITH DISTURBANCE, $C_{A_b} = 2 \cdot 25$

FIG.6.

FIG. 7.

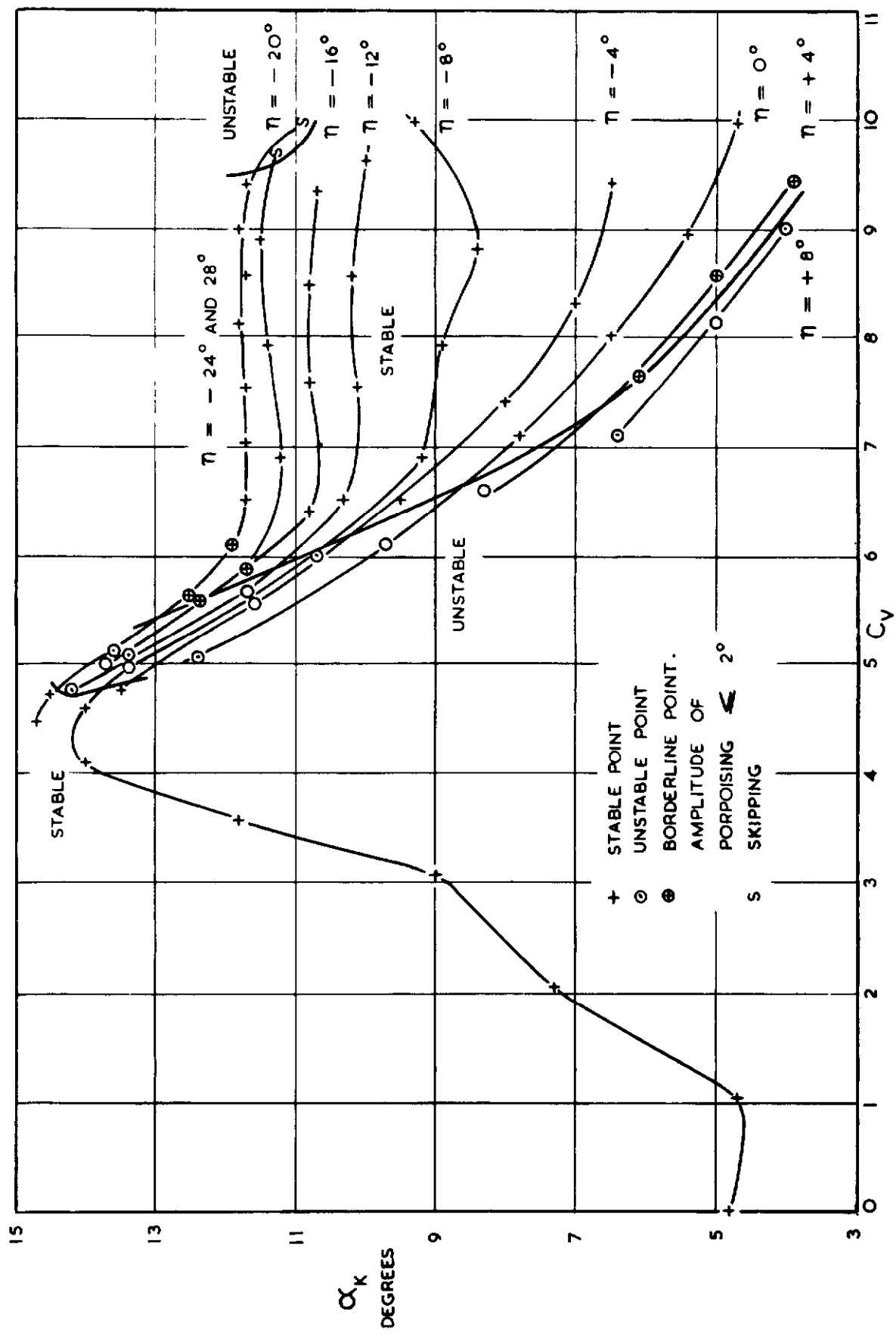

MODEL J
LONGITUDINAL STABILITY WITHOUT DISTURBANCE, $C_{\Delta_0} = 2 \cdot 75$

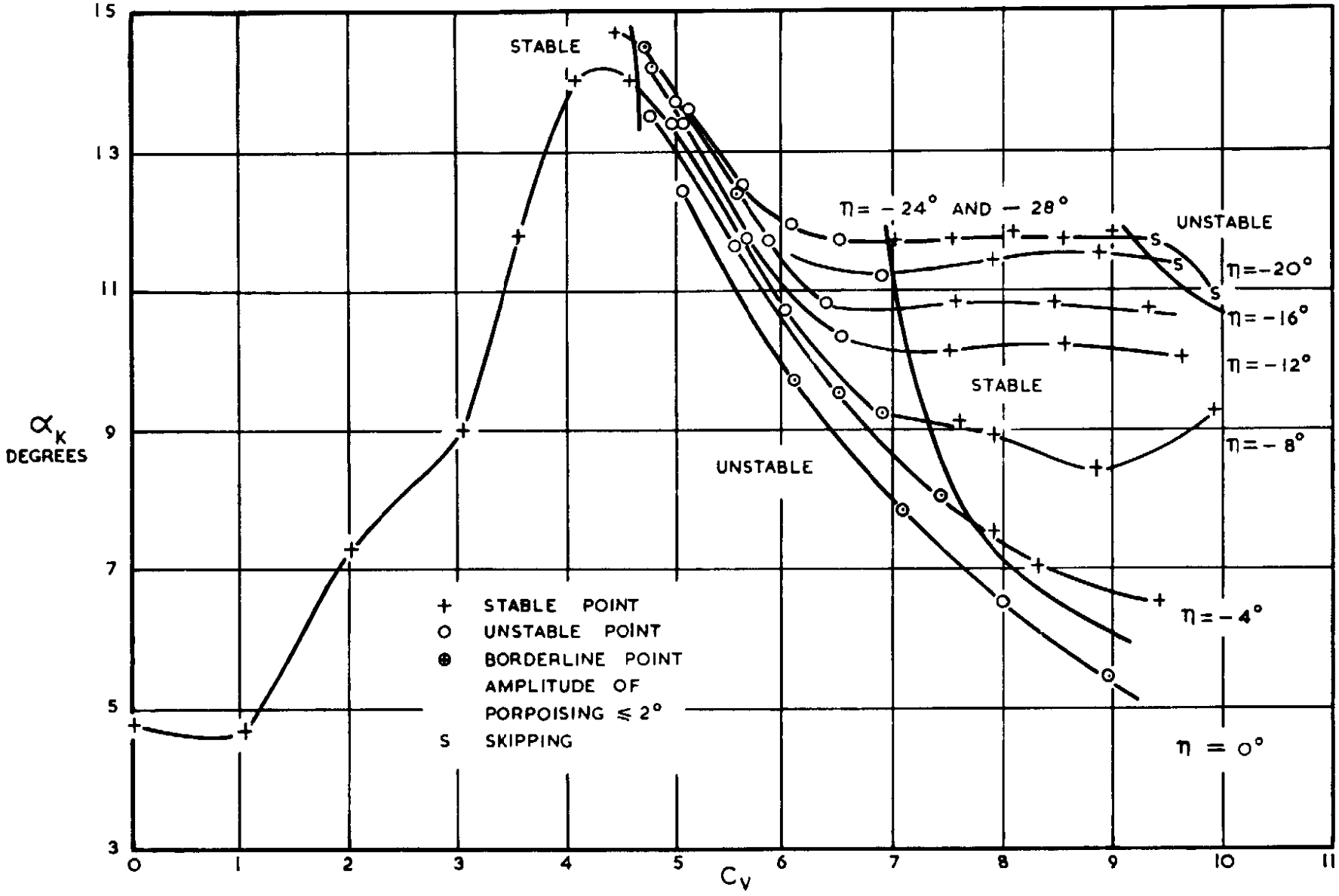

MODEL J

LONGITUDINAL STABILITY WITH DISTUIBANCE, $C_{\Delta_0} = 2 \cdot 75$

FIG. 8.

FIG. 9.

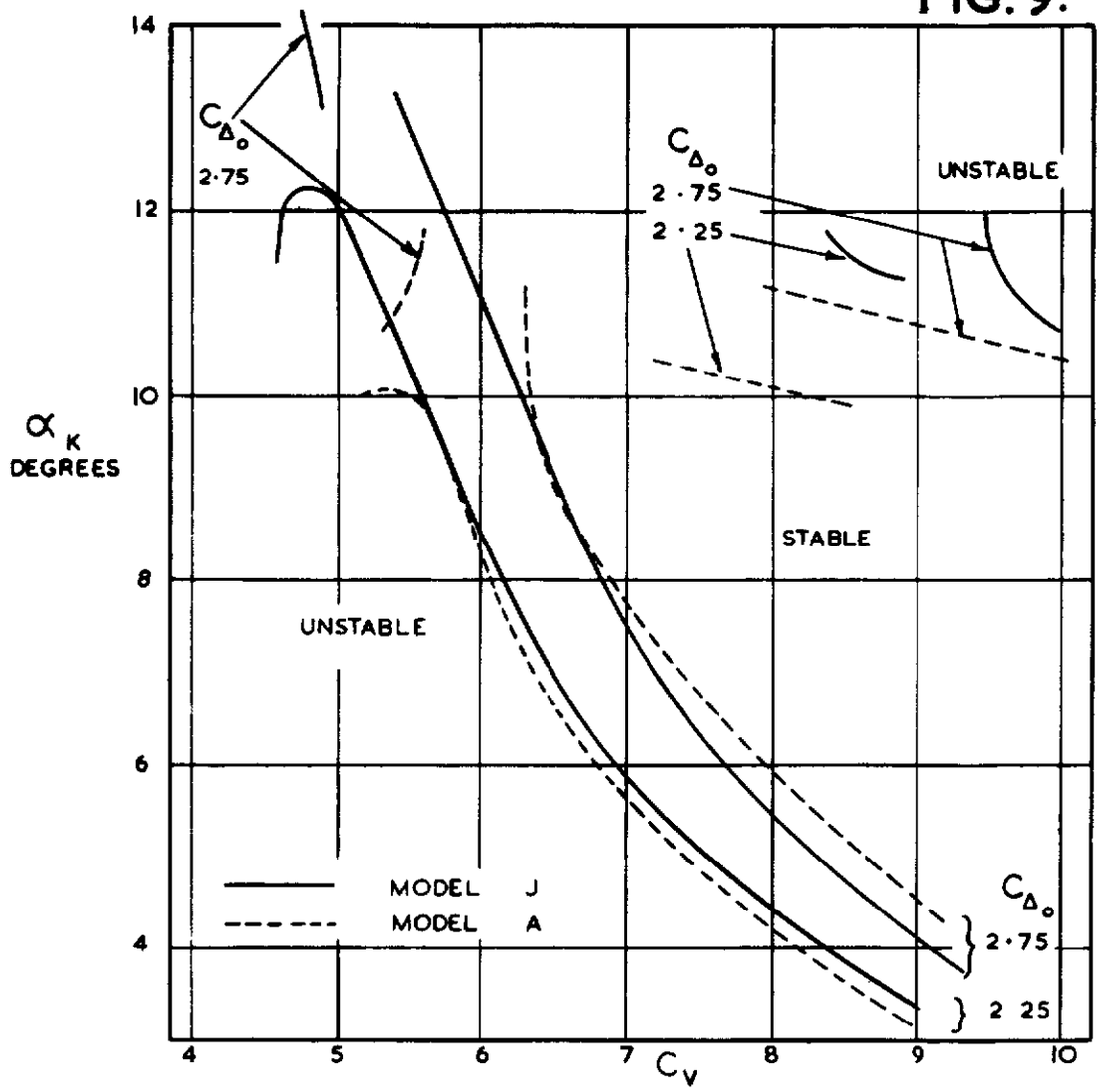

(a) UNDISTURBED

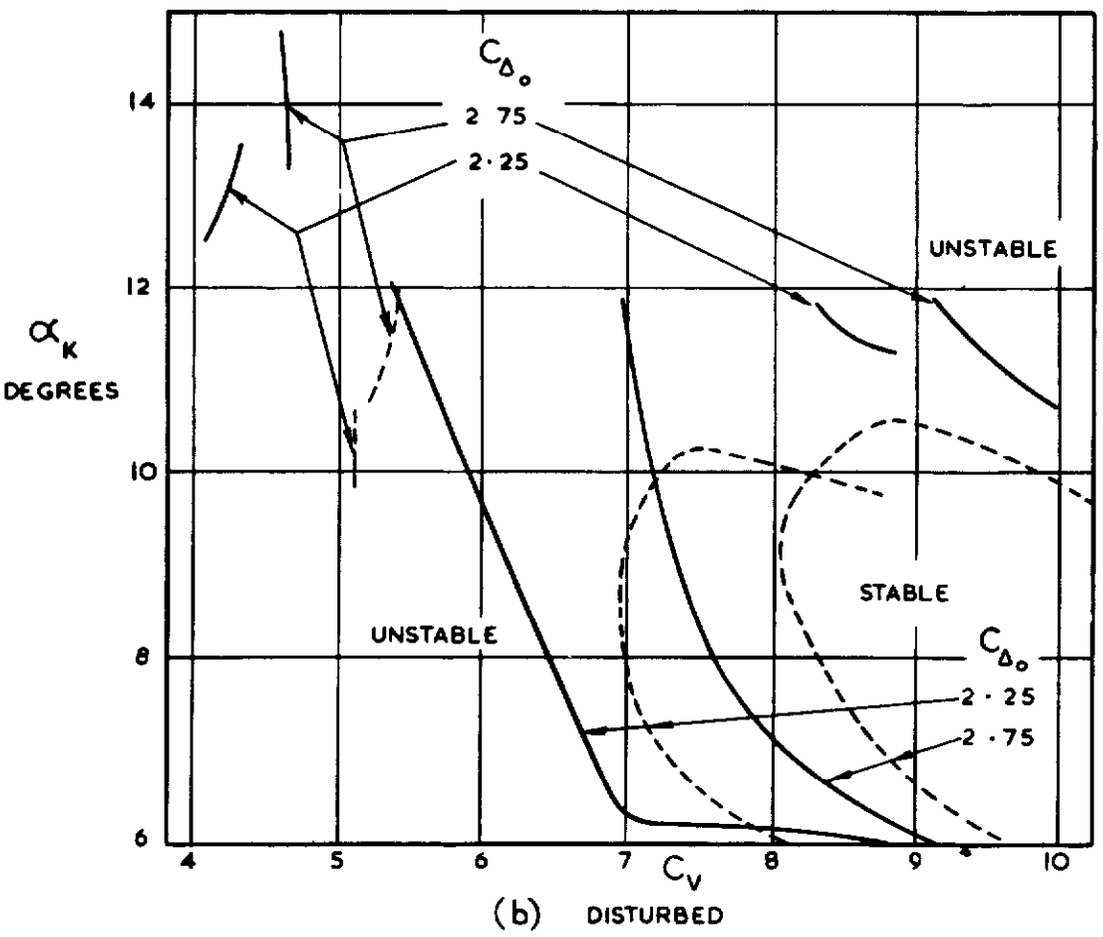

(b) DISTURBED

EFFECT OF A TAILORED AFTERBODY ON LONGITUDINAL STABILITY LIMITS

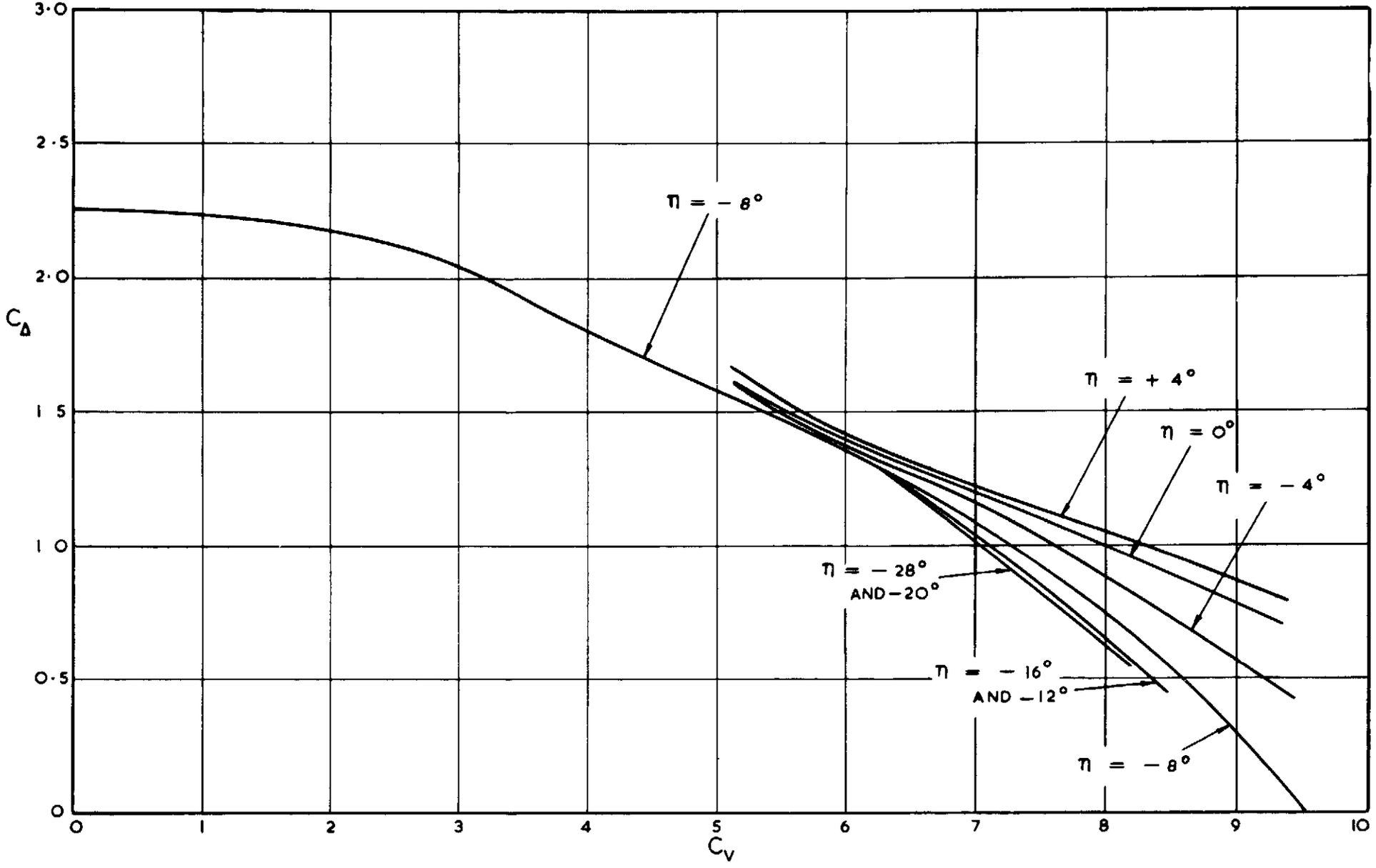

MODEL J
LOAD COEFFICIENT CURVES, $C_{\Delta_o} = 2{\cdot}25$

FIG. 10.

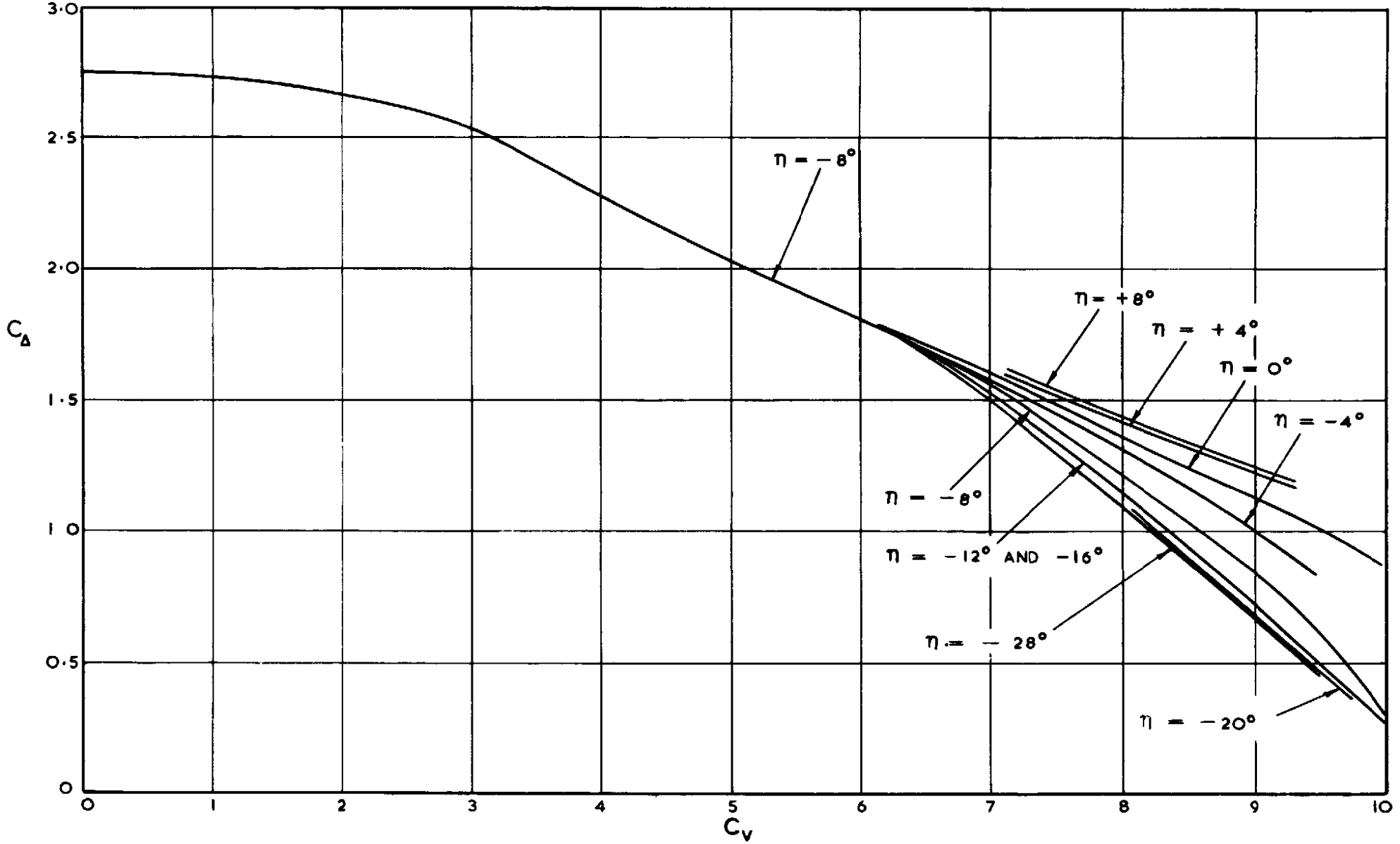

MODEL J

LOAD COEFFICIENT CURVES, $C_{\Delta_o} = 2 \cdot 75$

FIG.11.

FIG.12

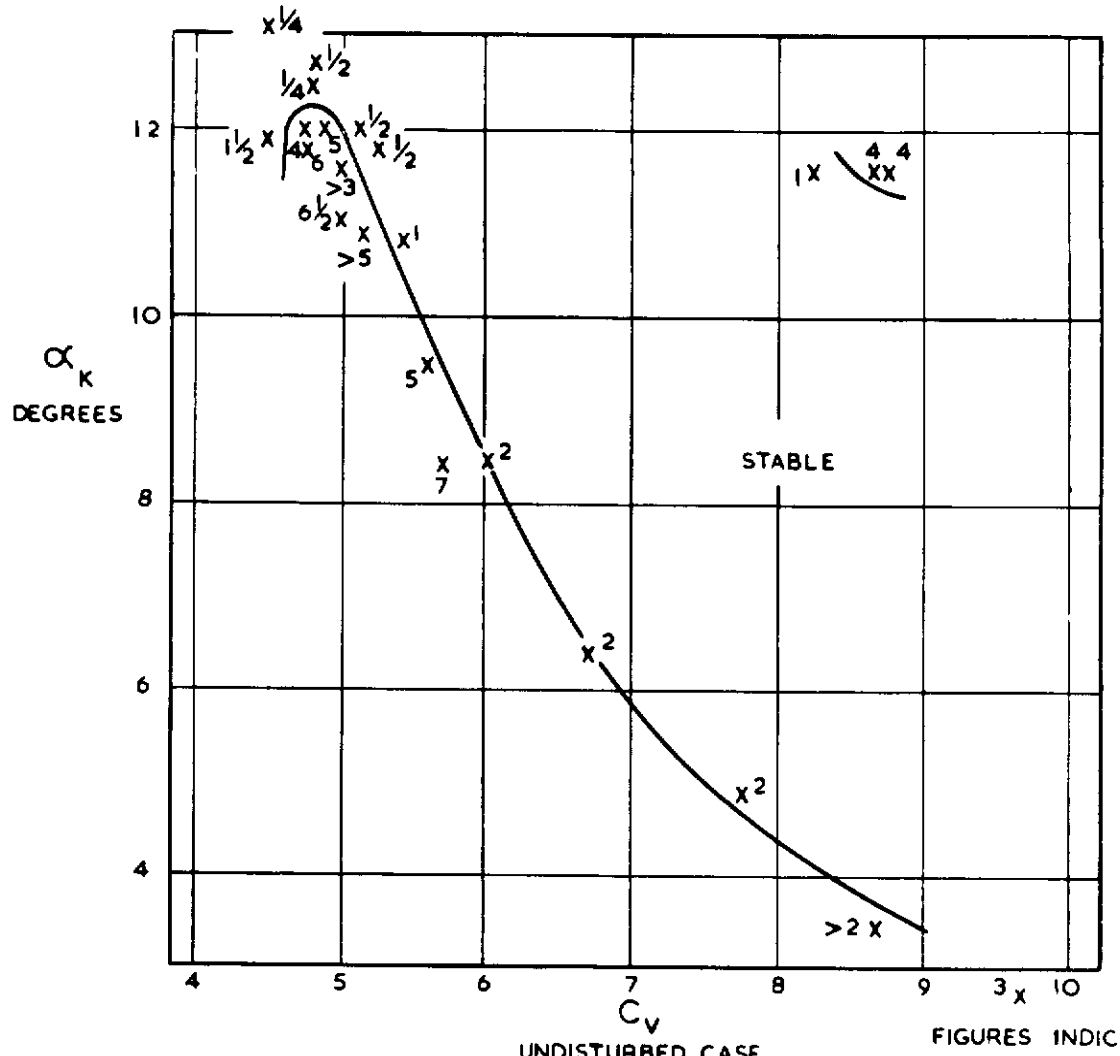

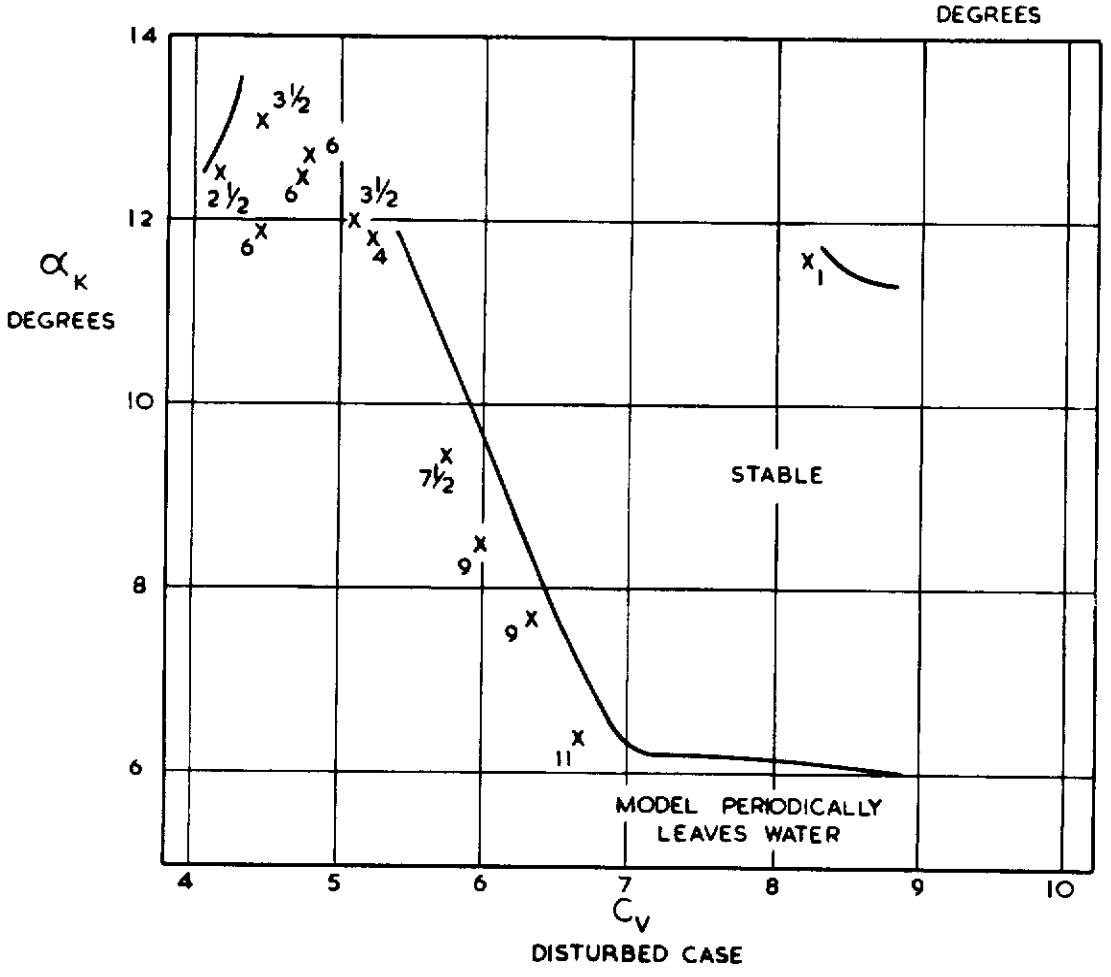

MODEL J

PORPOISING AMPLITUDES AND STABILITY LIMITS, $C_{\Delta_0} = 2{\cdot}25$

FIG.13.

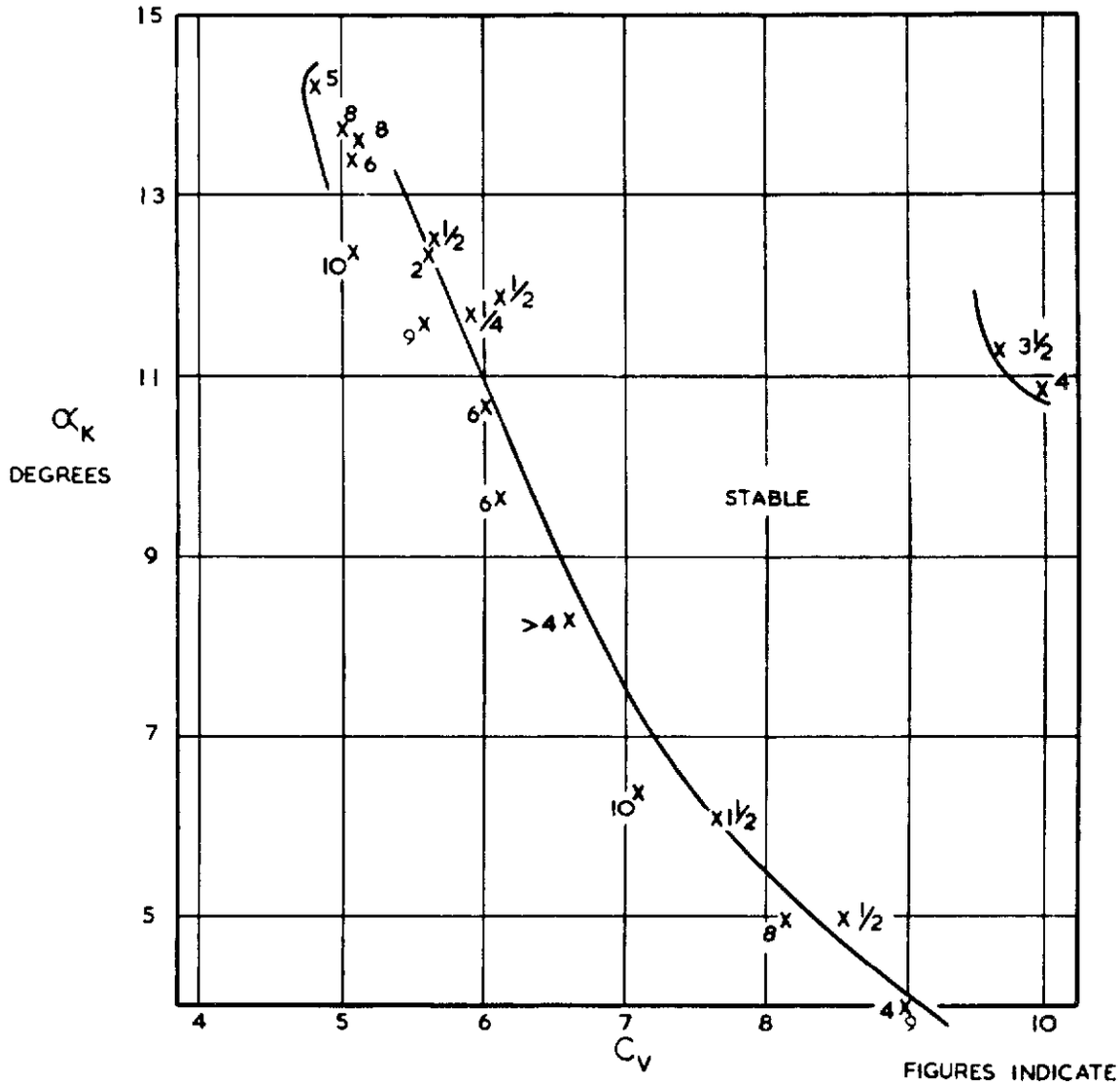

UNDISTURBED CASE

FIGURES INDICATE AMPLITUDES OF PORPOISING IN DEGREES

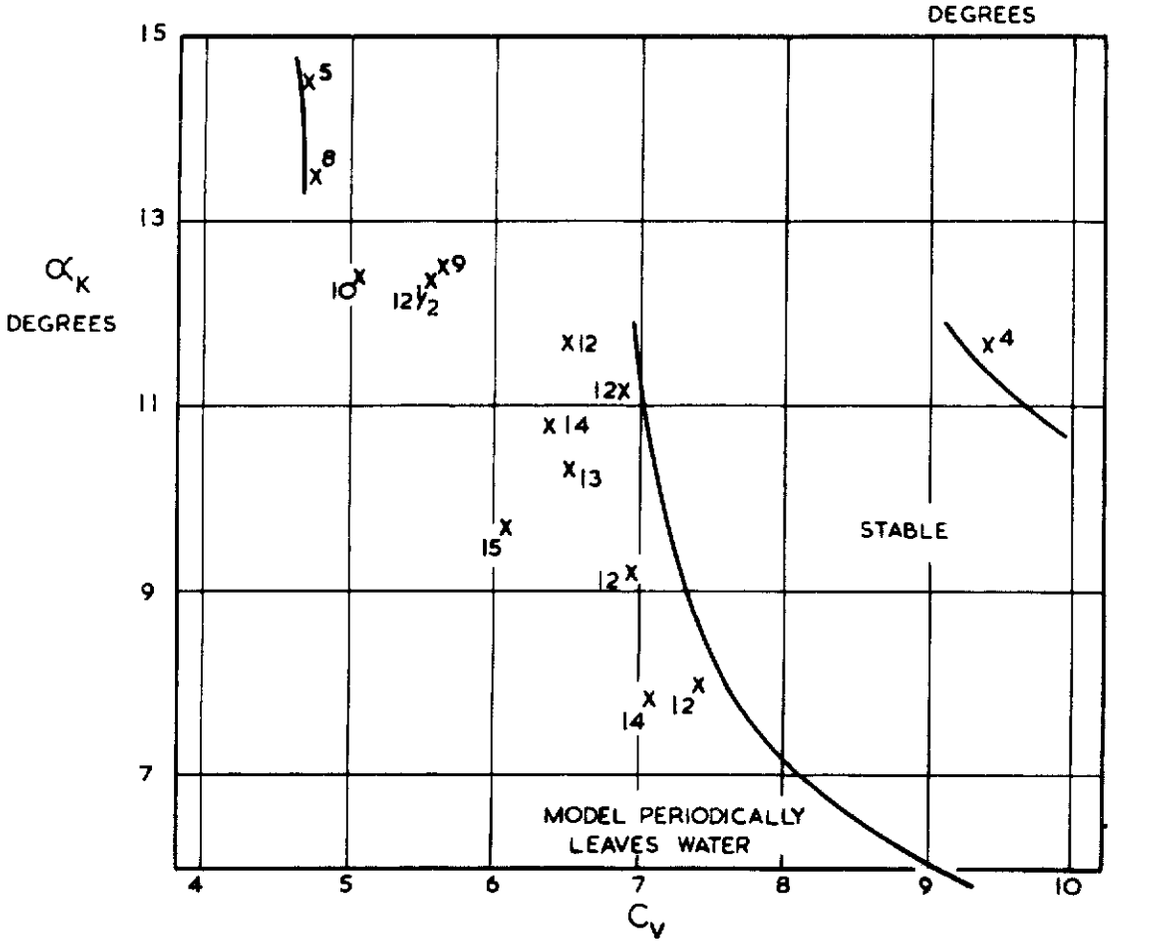

DISTURBED CASE

MODEL J

PORPOISING AMPLITUDES AND STABILITY LIMITS, $C_{\Delta_o}=2{\cdot}75$

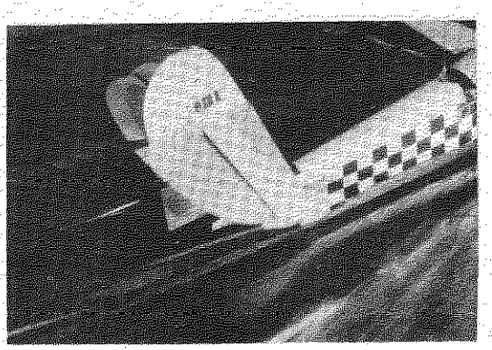

(a)
$\eta = -24°$
$C_v = 5{\cdot}68$
$\alpha_K = 11{\cdot}4°$

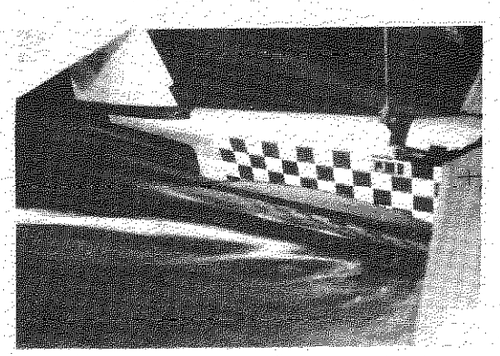

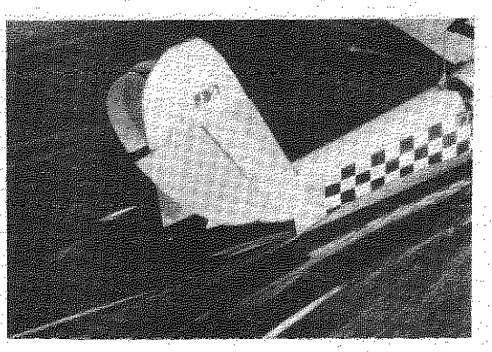

(b)
$\eta = -4°$
$C_v = 5{\cdot}7$
$\alpha_K = 9{\cdot}6°$

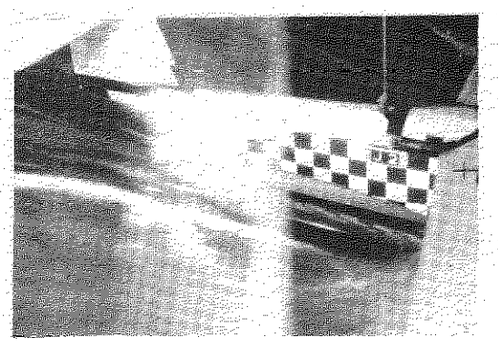

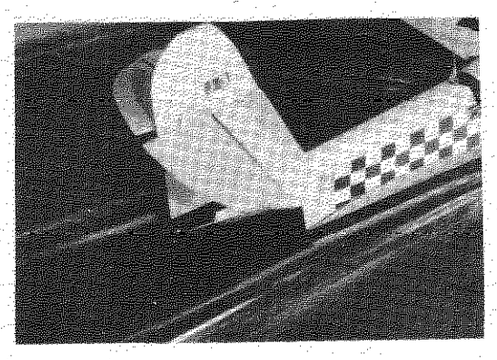

(c)
$\eta = -8°$
$C_v = 6{\cdot}93$
$\alpha_K = 8{\cdot}9°$

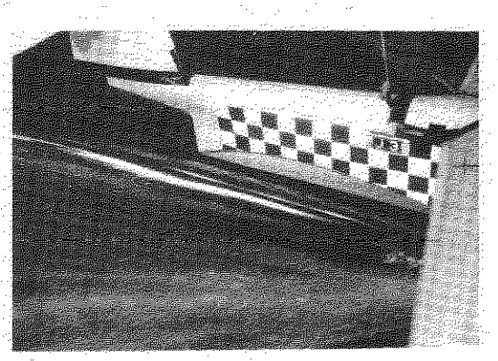

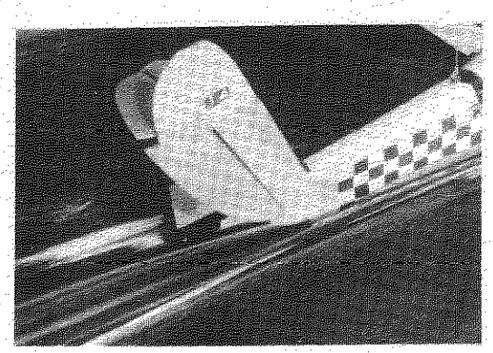

(d)
$\eta = -20°$
$C_v = 8{\cdot}14$
$\alpha_K = 11{\cdot}2°$

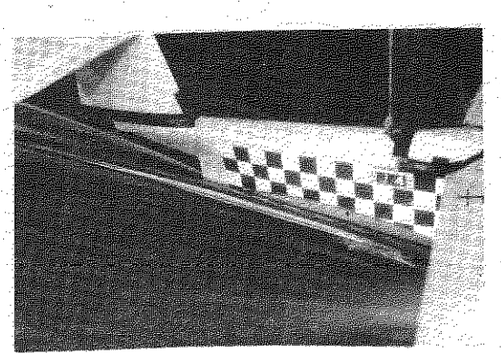

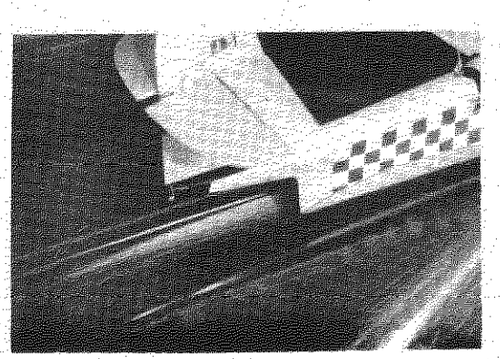

(e)
$\eta = 0°$
$C_v = 9{\cdot}16$
$\alpha_K = 4{\cdot}1°$

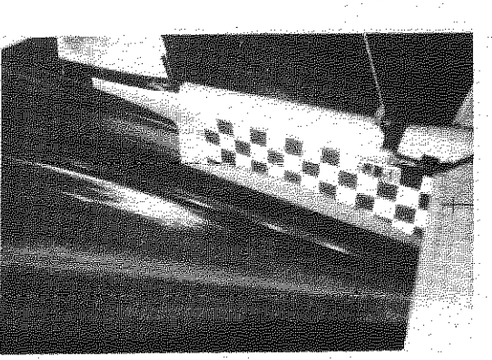

MODEL J

WAKE PHOTOGRAPHS

$C_{\Delta_o} = 2{\cdot}25$

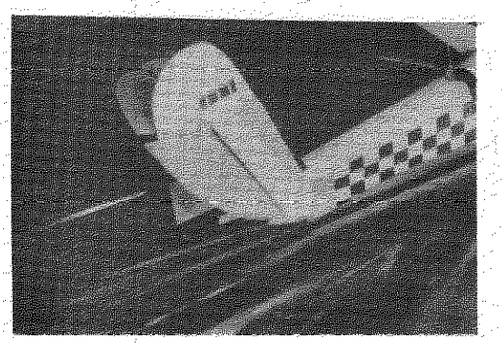

(a)
$\eta = -24°$
$C_v = 6{\cdot}65$
$\alpha_k = 11{\cdot}7°$

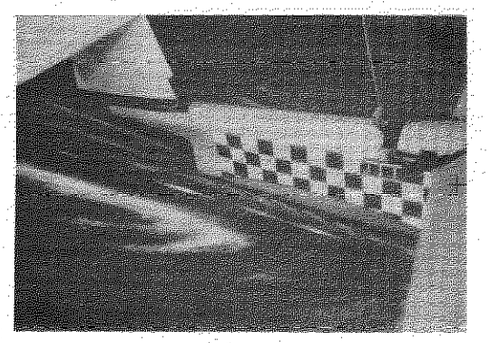

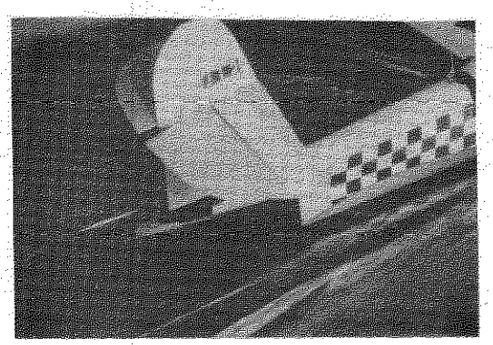

(b)
$\eta = 0°$
$C_v = 7{\cdot}18$
$\alpha_k = 7{\cdot}7°$

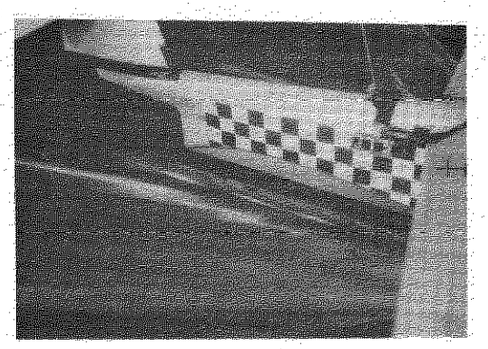

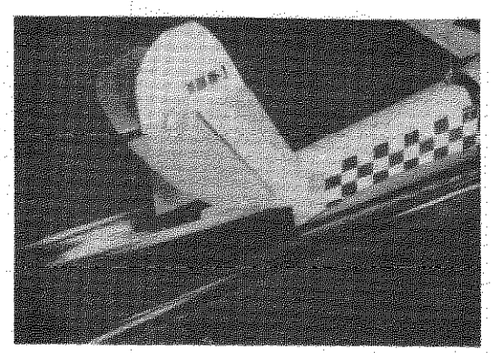

(c)
$\eta = -8°$
$C_v = 8{\cdot}19$
$\alpha_k = 8{\cdot}7°$

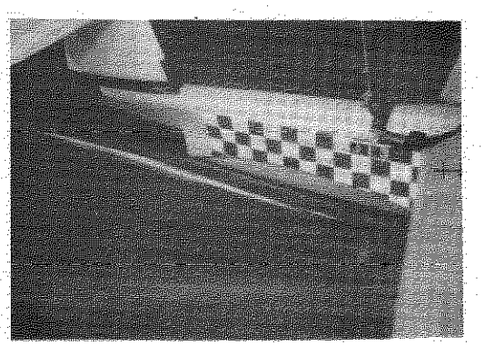

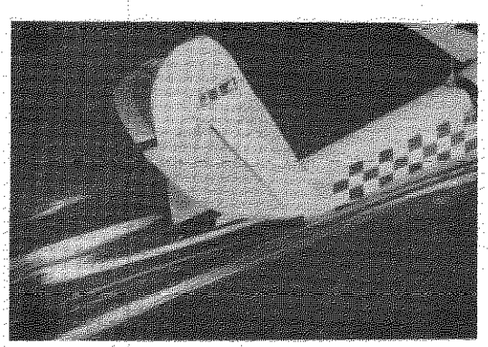

(d)
$\eta = -12°$
$C_v = 9{\cdot}16$
$\alpha_k = 10{\cdot}1°$

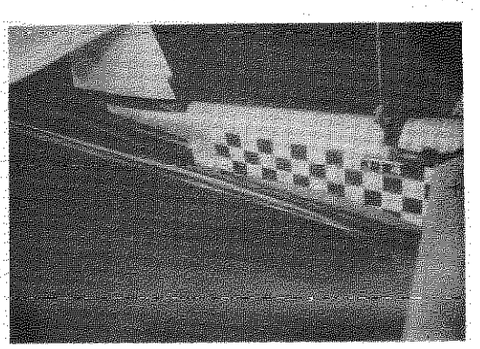

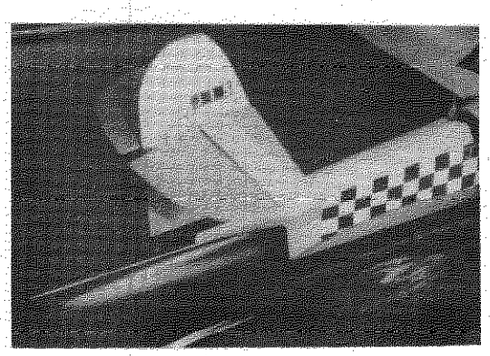

(e)
$\eta = 0°$
$C_v = 9{\cdot}16$
$\alpha_k = 5{\cdot}2°$

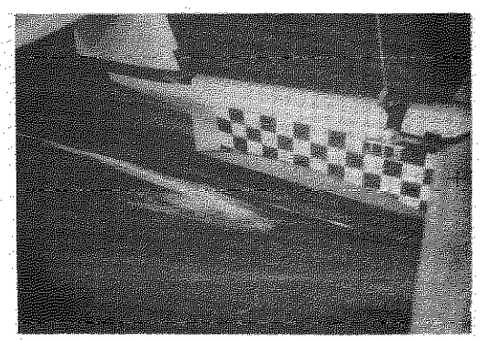

MODEL J

WAKE PHOTOGRAPHS

$C_{\Delta_o} = 2{\cdot}75$

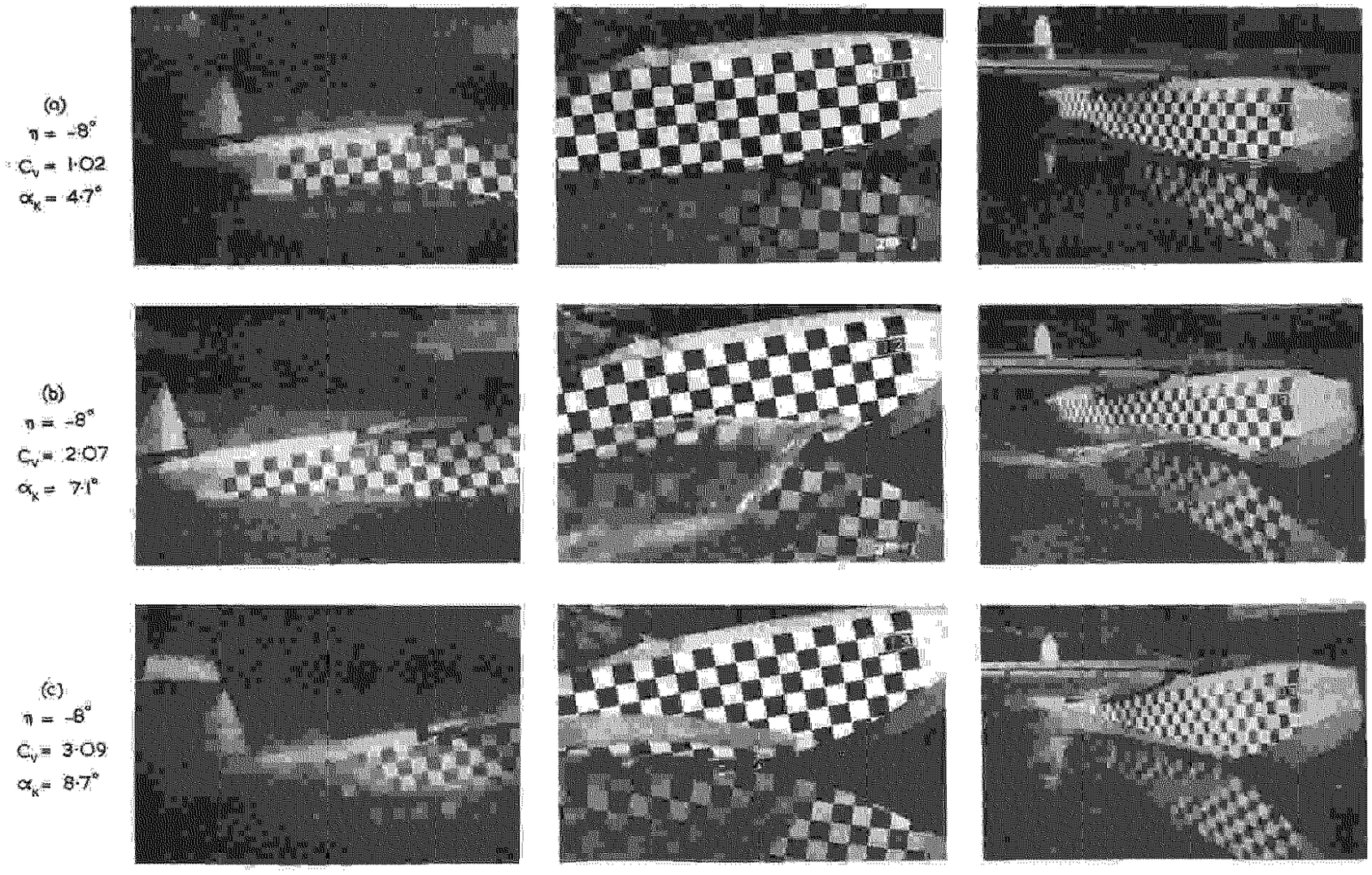

MODEL J

SPRAY PHOTOGRAPHS, C_{D_s}=2·25, (1)

FIG.16

(a)
$\eta = -8°$
$C_v = 3{\cdot}63$
$\alpha_K = 12{\cdot}0°$

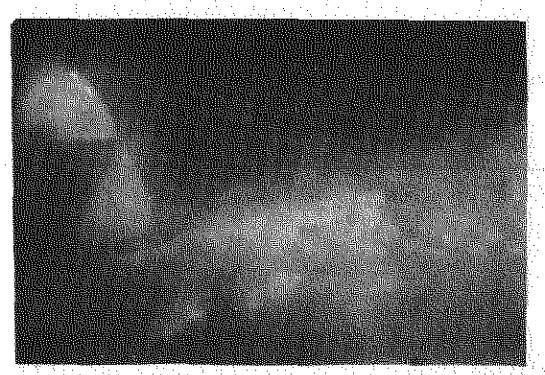

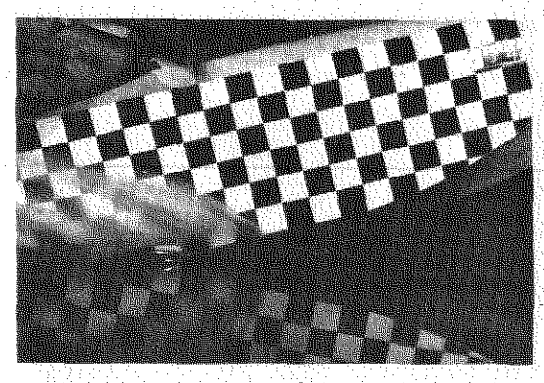

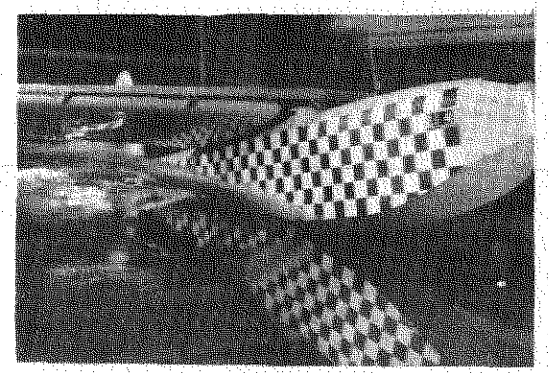

(b)
$\eta = -8°$
$C_v = 4{\cdot}09$
$\alpha_K = 12{\cdot}8°$

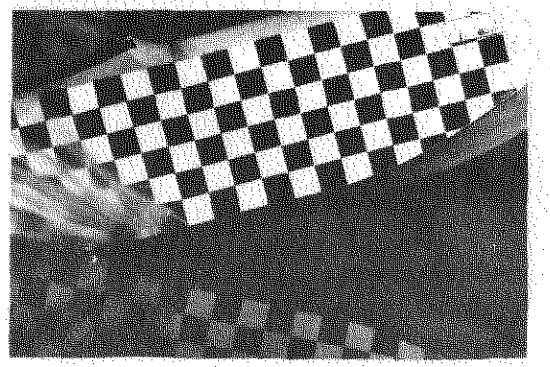

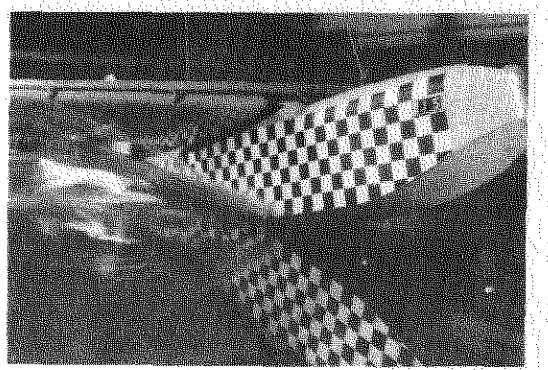

(c)
$\eta = -8°$
$C_v = 7{\cdot}11$
$\alpha_K = 8{\cdot}8°$

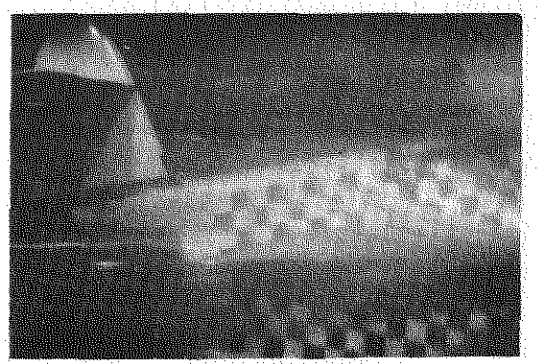

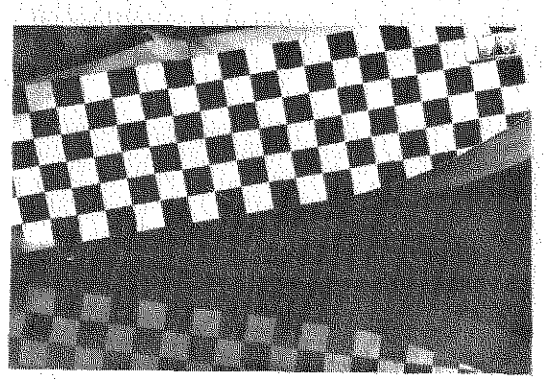

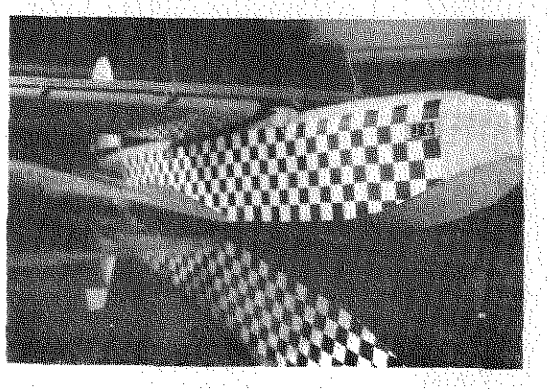

MODEL J

SPRAY PHOTOGRAPHS, $C_{\Delta_0} = 2{\cdot}25$, (2)

FIG.17

(a)
$\eta = -8°$
$C_v = 1{\cdot}02$
$\alpha_k = 4{\cdot}7°$

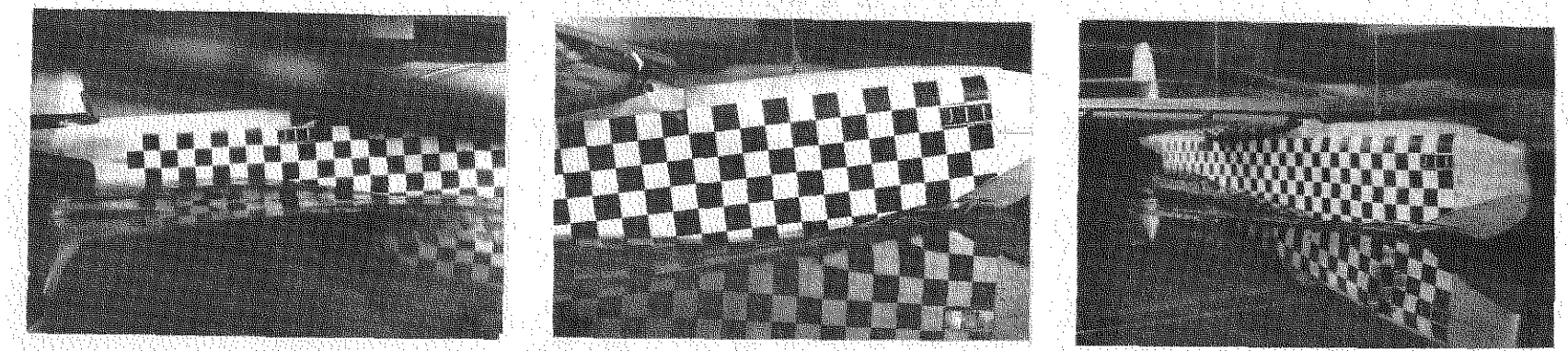

(b)
$\eta = -8°$
$C_v = 2{\cdot}05$
$\alpha_k = 7{\cdot}3°$

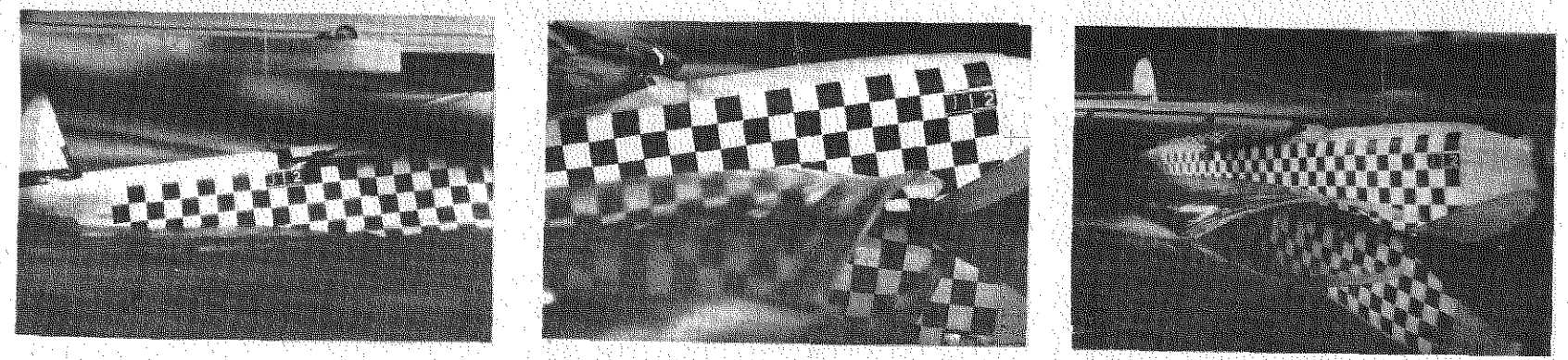

(c)
$\eta = -8°$
$C_v = 3{\cdot}12$
$\alpha_k = 9{\cdot}2°$

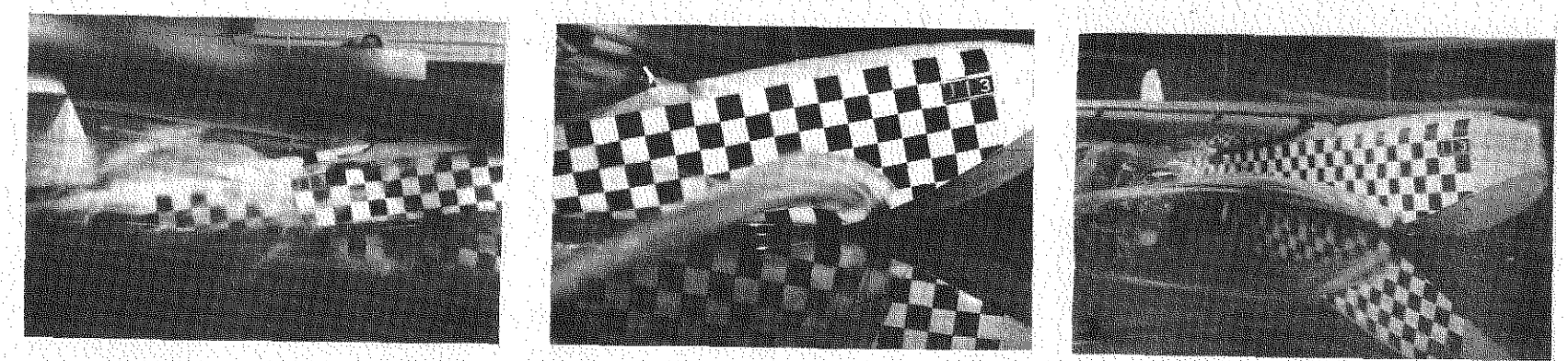

MODEL J

SPRAY PHOTOGRAPHS, $C_{\Delta_o} = 2{\cdot}75$, (1)

FIG. 18

(a)
$\eta = -8°$
$C_v = 3{\cdot}63$
$\alpha_k = 12{\cdot}0°$

(b)
$\eta = -8°$
$C_v = 4{\cdot}14$
$\alpha_k = 14{\cdot}1°$

(c)
$\eta = -8°$
$C_v = 8{\cdot}19$
$\alpha_k = 8{\cdot}8°$

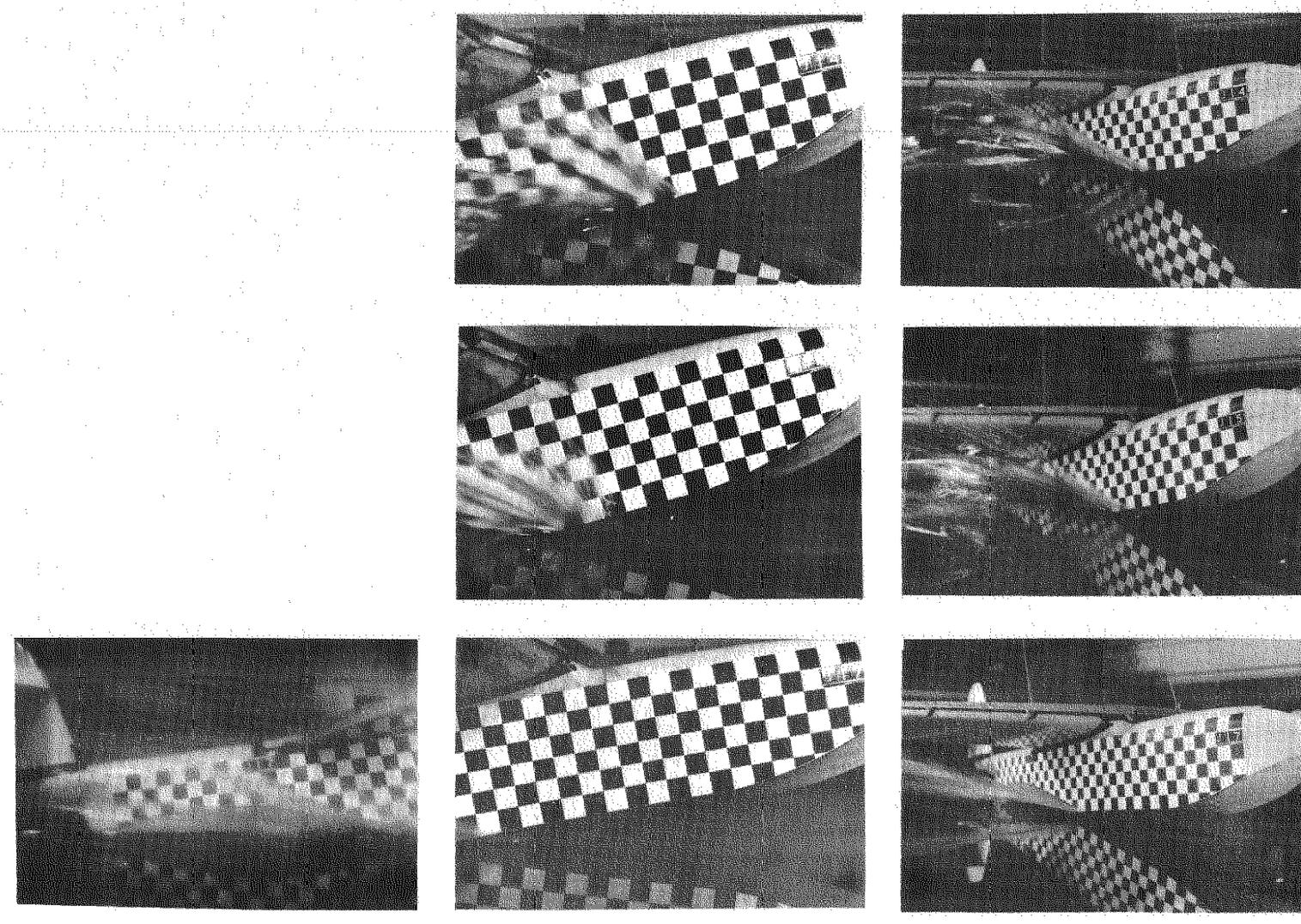

MODEL J

SPRAY PHOTOGRAPHS, $C_{\Delta_o} = 2{\cdot}75$, (2)

FIG. 19

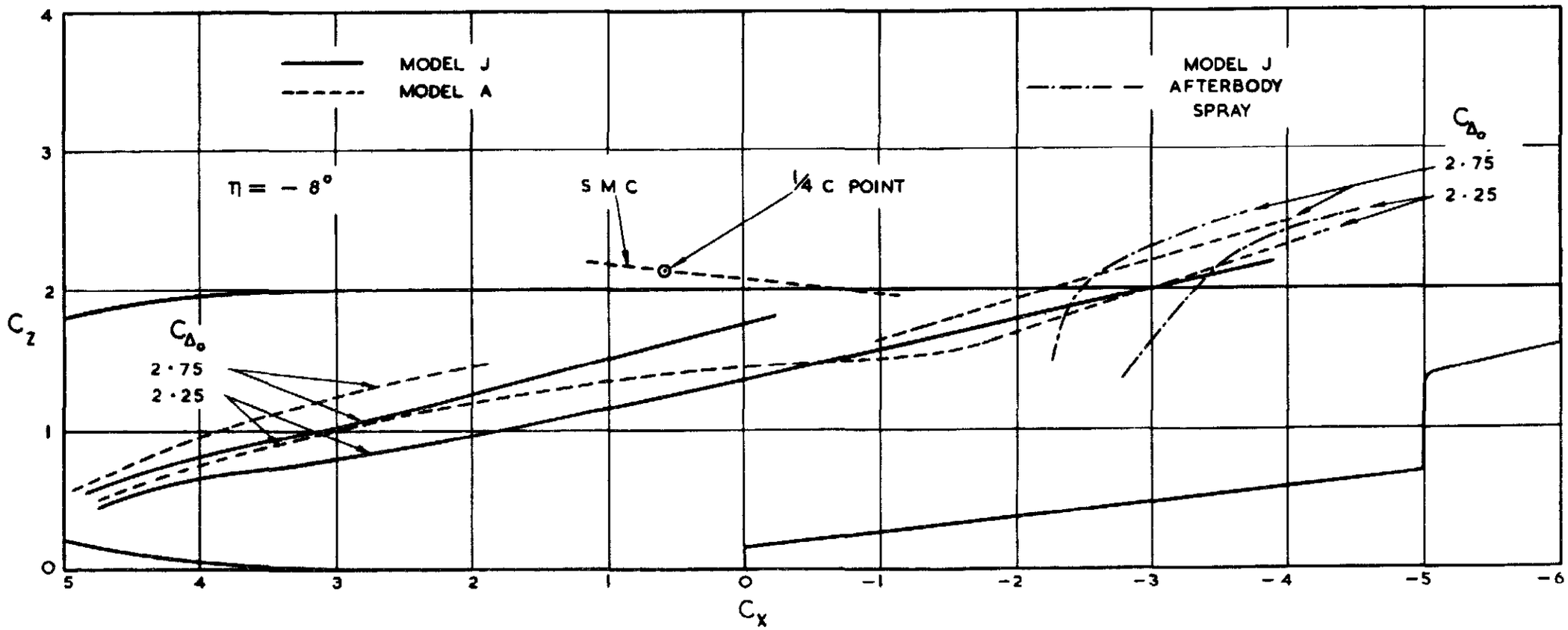

FIG. 20

MODEL J.
EFFECT OF A TAILORED AFTERBODY ON SPRAY PROJECTIONS.

FIG. 21.

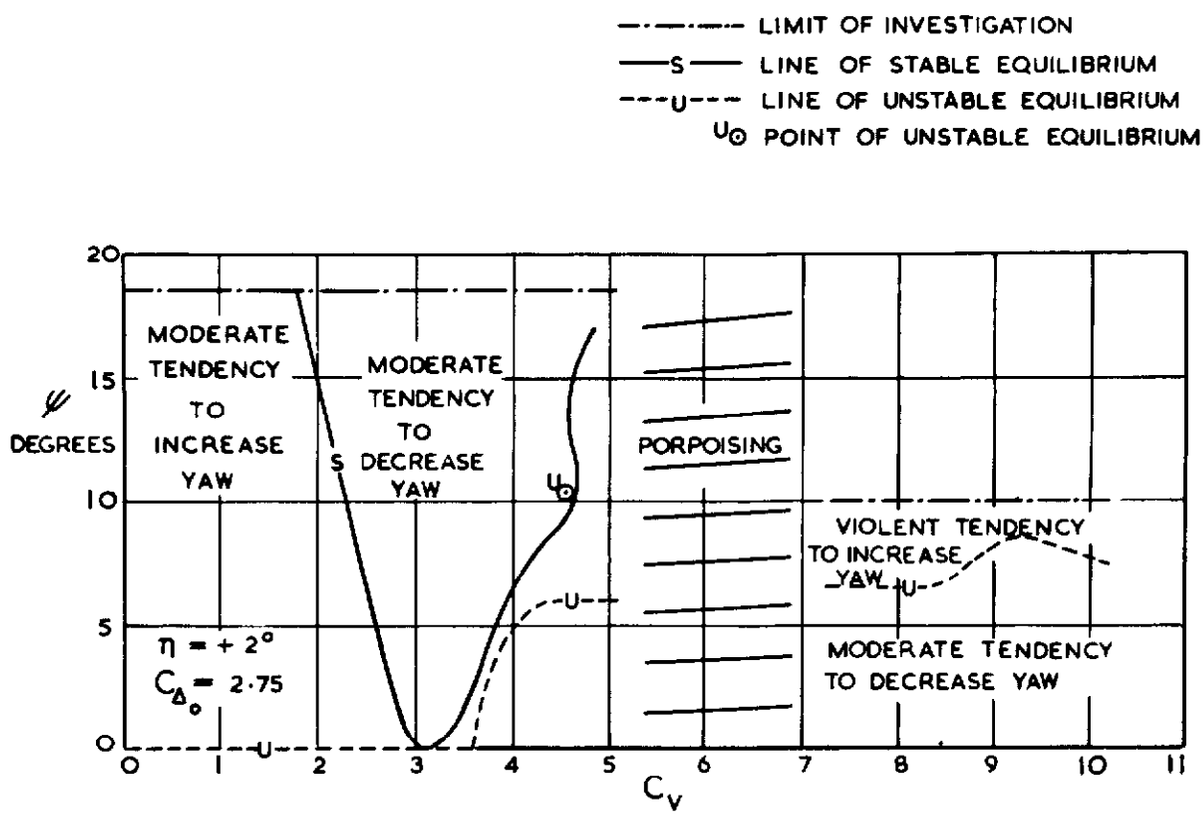

(a) NORMAL AFTERBODY

MODEL A

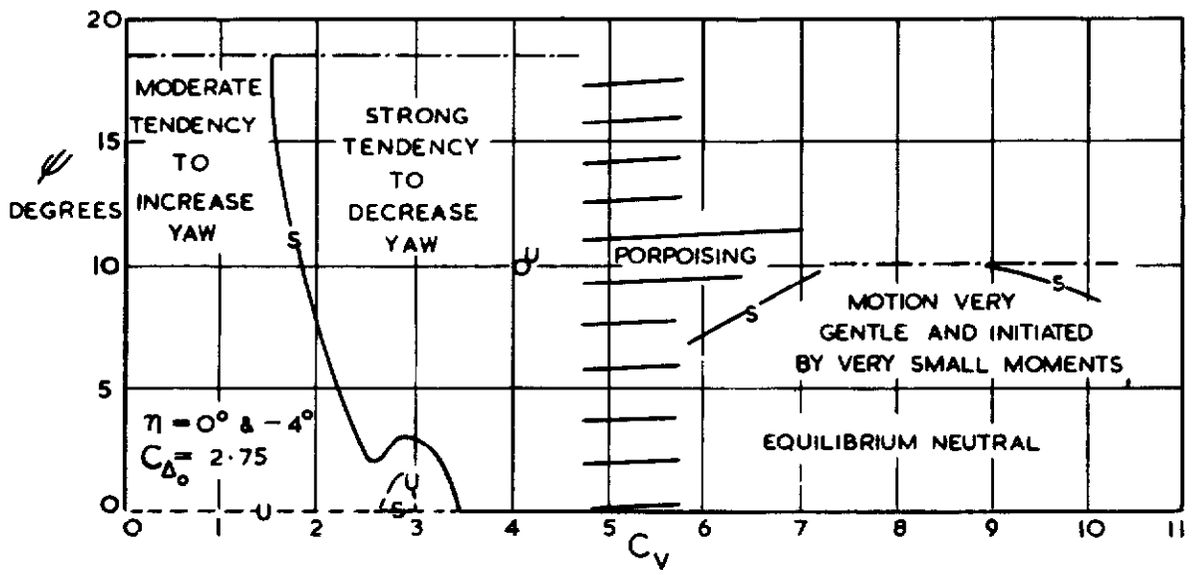

(b) TAILORED AFTERBODY

MODEL J

EFFECT OF TAILORED AFTERBODY ON DIRECTIONAL STABILITY, $C_{V_o} = 2.75$

FIG.22.

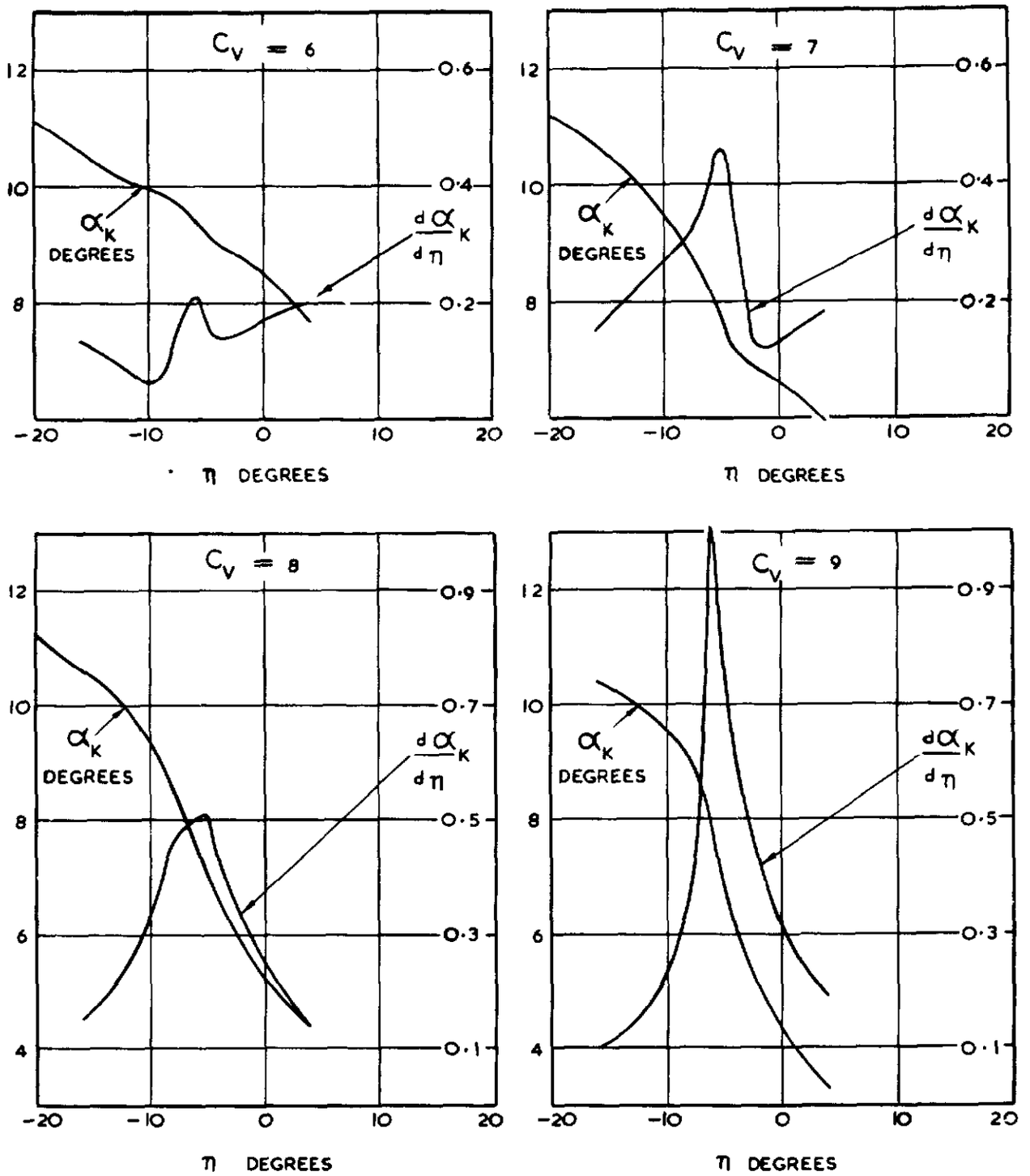

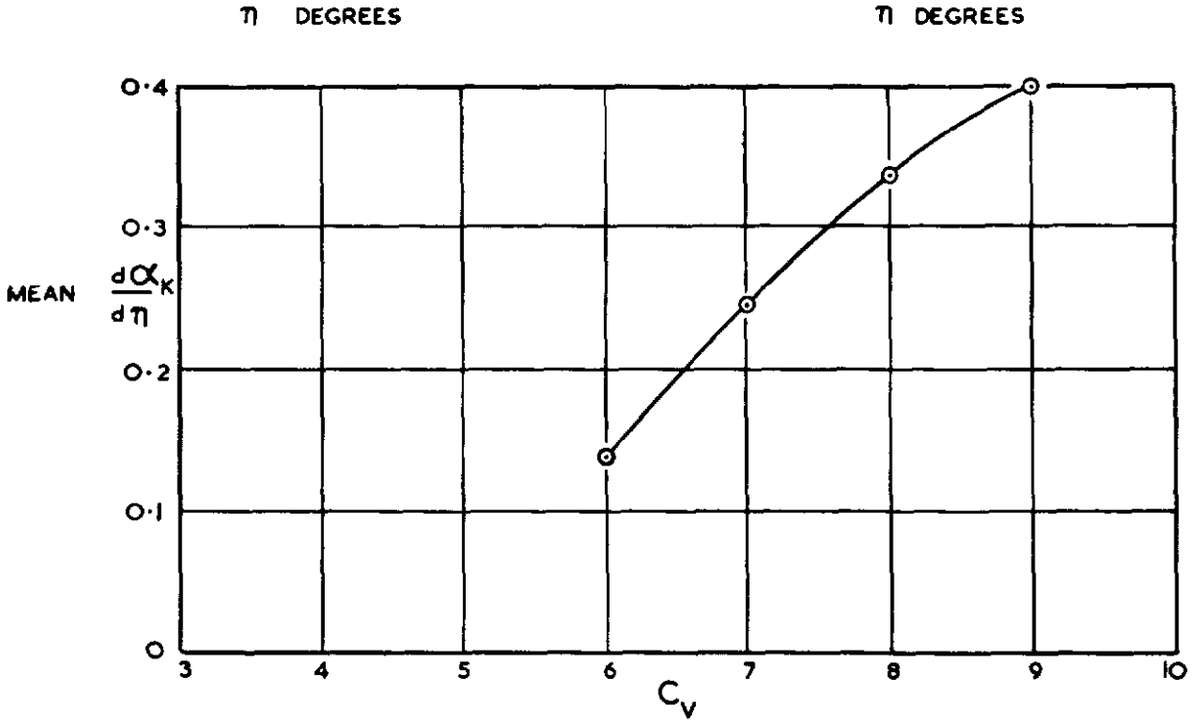

MODEL J

ELEVATOR EFFECTIVENESS C_{Δ_0} -2·25

FIG.23.

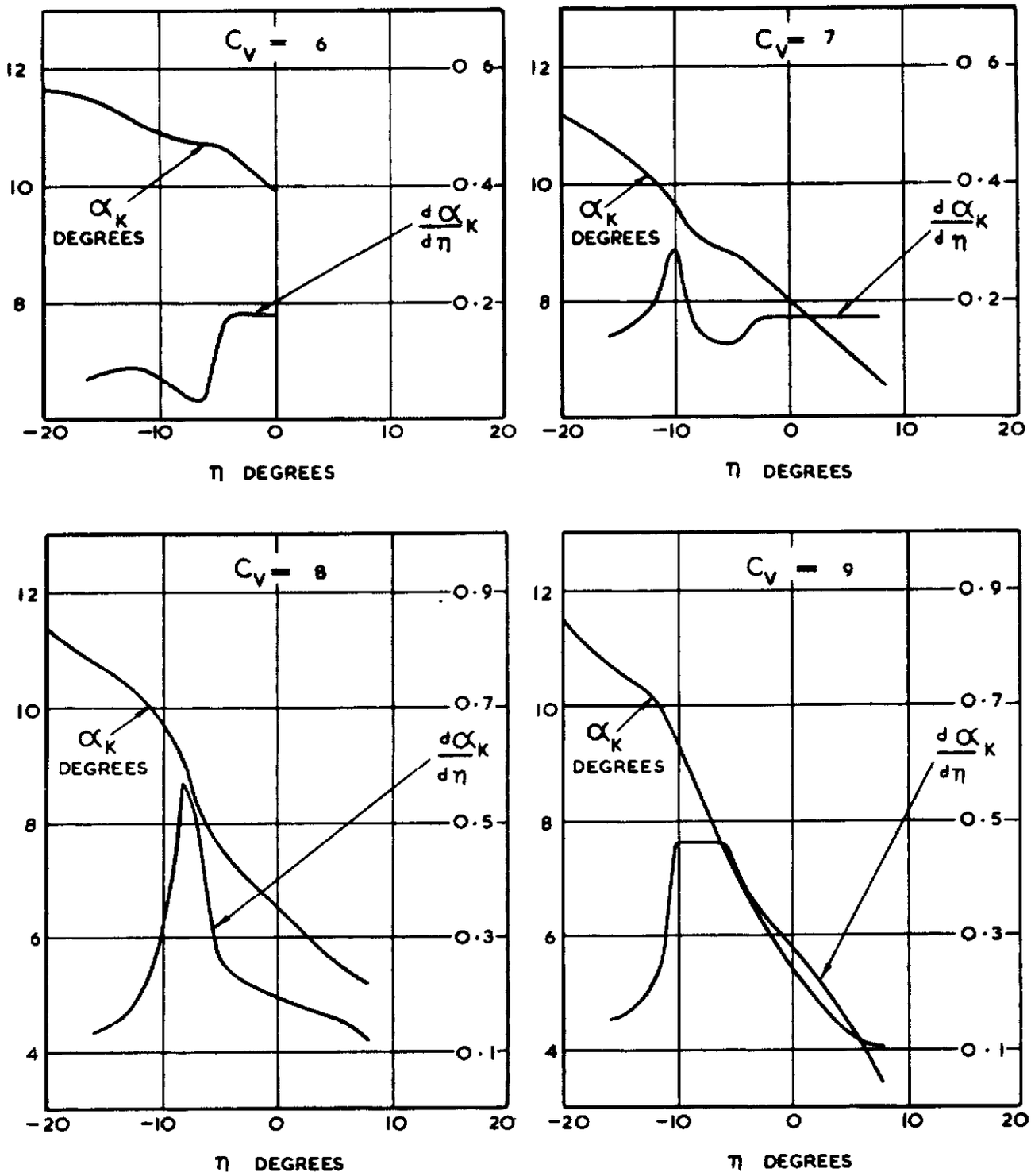

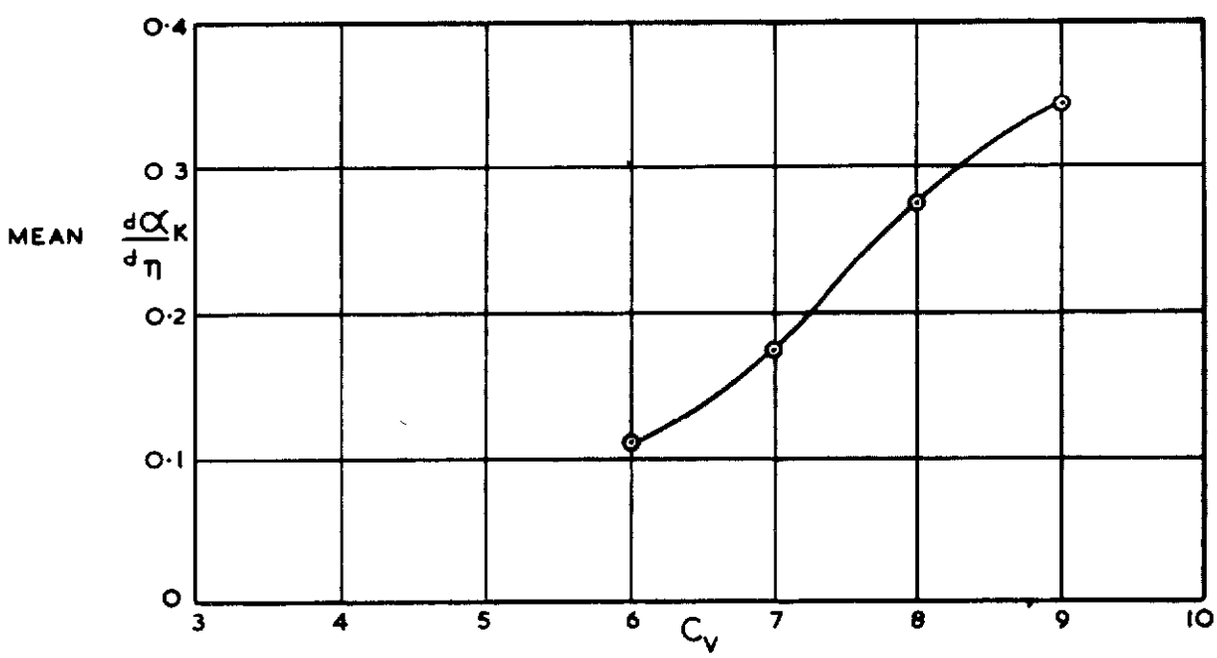

MODEL J

ELEVATOR EFFECTIVENESS, C_{Δ_o} = 2·75

FIGS. 24 & 25.

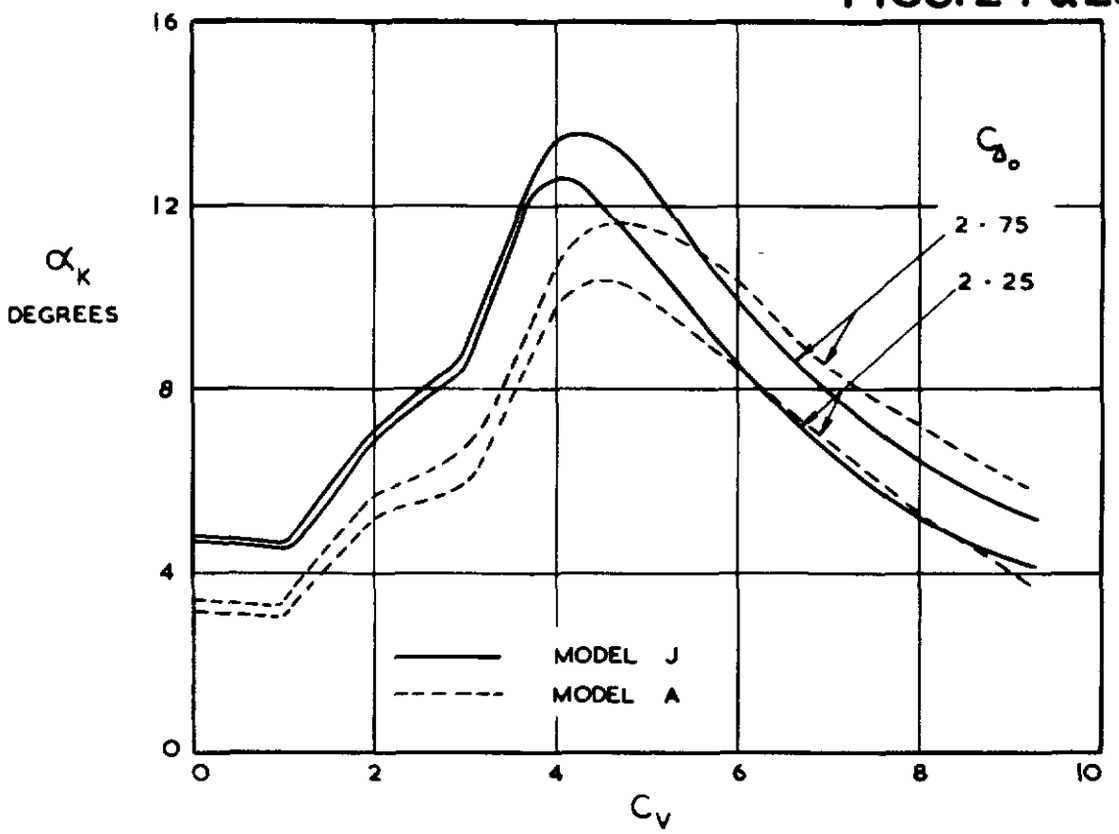

FIG. 107. EFFECT OF A TAILORED AFTERBODY ON TRIM CURVES

$\eta = 0°$

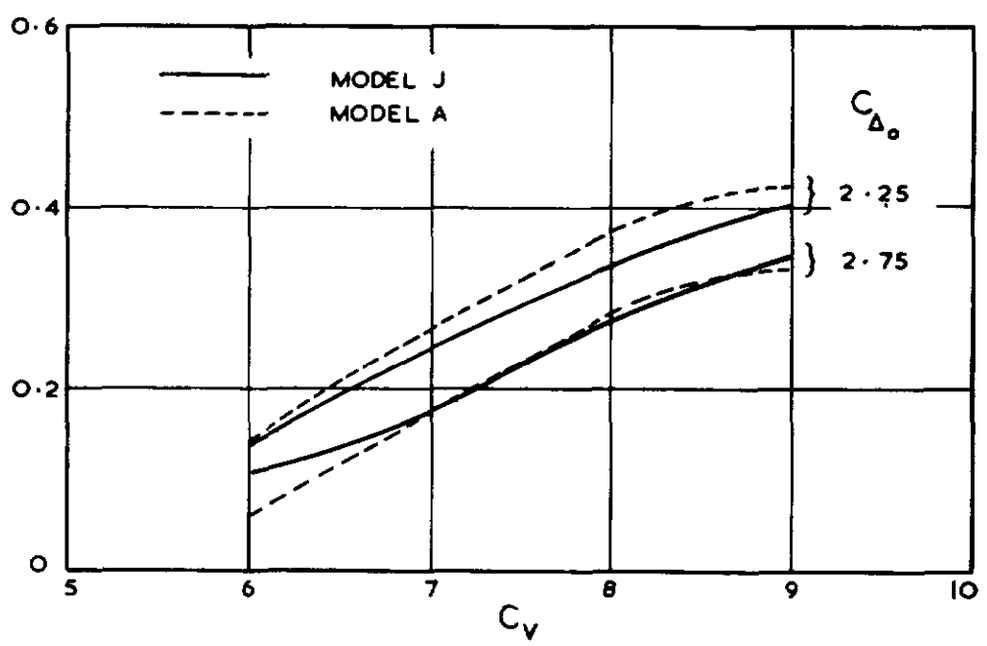

FIG. 108. EFFECT OF A TAILORED AFTERBODY ON ELEVATOR EFFECTIVENESS

629.135.52

D.M. RIDLAND

INVESTIGATION OF HIGH LENGTh/BEAM RATIO SEAPLANE HULLS WITH HIGH BEAM LOADINGS

HYDRODYNAMIC STABILITY PART 14

THE EFFECT OF A TAILORED AFTERBODY ON STABILITY AND SPRAY CHARACTERISTICS WITH TEST DATA ON MODEL J

2. 3.4
2.10.1
2.10.3

The effects of a tailored afterbody on longitudinal stability, spray, directional stability and elevator effectiveness are deduced from the results of tests on two models of length/beam ratio 11, which were alike in every respect except that of afterbody shape; one afterbody was of standard form and the other was tailored.

It was found that tailoring the afterbody considerably improved stability characteristics, both longitudinal and directional, improved spray characteristics and slightly impaired elevator effectiveness.

The detailed test results for the tailored afterbody model are also included and discussed.

629.135.52

D.M. RIDLAND

INVESTIGATION OF HIGH LENGTP/BEAM RATIO SEAPLANE HULLS WITH HIGH BEAM LOADINGS

HYDRODYNAMIC STABILITY PART 14

THE EFFECT OF A TAILORED AFTERBODY ON STABILITY AND SPRAY CHARACTERISTICS WITH TEST DATA ON MODEL J

2. 3.4
2.10.1
2.10.3

The effects of a tailored afterbody on longitudinal stability, spray, directional stability and elevator effectiveness are deduced from the results of tests on two models of length/beam ratio 11, which were alike in every respect except that of afterbody shape; one afterbody was of standard form and the other was tailored.

It was found that tailoring the afterbody considerably improved stability characteristics, both longitudinal and directional, improved spray characteristics and slightly impaired elevator effectiveness.

The detailed test results for the tailored afterbody model are also included and discussed.

629.135.52

D.M. RIDLAND

INVESTIGATIGATION OF HIGH LENGTH/BEAM RATIO SEAPLANE HULLS WITH HIGH BEAM LOADINGS

HYDRODYNAMIC STABILITY PART 14

THE EFFECT OF A TAILORED AFTERBODY ON STABILITY AND SPRAY CHARACTERISTICS WITH TEST DATA ON MODEL J

2. 3.4
2.10.1
2.10.3

The effects of a tailored afterbody on longitudinal stability, spray, directional stability and elevator effectiveness are deduced from the results of tests on two models of length/beam ratio 11, which were alike in every respect except that of afterbody shape; one afterbody was of standard form and the other was tailored.

It was found that tailoring the afterbody considerably improved stability characteristics, both longitudinal and directional, improved spray characteristics and slightly impaired elevator effectiveness.

The detailed test results for the tailored afterbody model are also included and discussed.

629.135.52

D.M. RIDLAND

INVESTIGATION OF HIGH LENGTH/BEAM RATIO SEAPLANE HULLS WITH HIGH BEAM LOADINGS

HYDRODYNAMIC STABILITY PART 14

THE EFFECT OF A TAILORED AFTERBODY ON STABILITY AND SPRAY CHARACTERISTICS WITH TEST DATA ON MODEL J

2. 3.4
2.10.1
2.10.3

The effects of a tailored afterbody on longitudinal stability, spray, directional stability and elevator effectiveness are deduced from the results of tests on two models of length/beam ratio 11, which were alike in every respect except that of afterbody shape; one afterbody was of standard form and the other was tailored.

It was found that tailoring the afterbody considerably improved stability characteristics, both longitudinal and directional, improved spray characteristics and slightly impaired elevator effectiveness.

The detailed test results for the tailored afterbody model are also included and discussed.

Printed and published by
HER MAJESTY'S STATIONERY OFFICE

To be purchased from
York House, Kingsway, London W.C.2
423 Oxford Street, London W.1
13A Castle Street, Edinburgh 2
109 St Mary Street, Cardiff
39 King Street, Manchester 2
Tower Lane, Bristol 1
2 Edmund Street, Birmingham 3
80 Chichester Street, Belfast
or through any bookseller

Printed in Great Britain

S.O. Code No. 23-9010-51